NUCLEAR FUSION IN CRYSTAL HYDRIDES OF LIGHT ELEMENTS

COLD FUSION

TECHNICAL NOTE

KEYWORDS: *nuclear fusion, high pressure, electrical screening*

GENNADY V. FEDOROVICH *Russian Academy of Sciences*
Theoretical Problems Department, Vesnina 12, Moscow 121002, Russia

Received December 26, 1991
Accepted for Publication July 24, 1992

A new physical object called the E-cell can be used as an appropriate catalyst to facilitate nuclear fusion reactions in solids. The E-cell is a radiation defect in a crystalline lattice of A_xH_y hydride [ordering number Z and mass number N of element A must be equal to one of the following pairs: (2,3), (3,6), (4,7), or (5,10)] formed by the capture of a thermal neutron in a crystal. Two features of hydrogen nuclear dynamics are of interest:

1. *suppression of the Coulomb barrier between hydrogen nuclei due to many-body screening effects*
2. *sufficient acceleration of hydrogen nuclei up to a few hundred electron-volts.*

Experimental research in this area may lead to the creation of equipment for the effective enhancement of the fusion rate to values that are of practical interest.

I. INTRODUCTION

Cold nuclear fusion of hydrogen isotopes has been an elusive goal in 20th-century physics. As early as 1940, Wildhack[1] conjectured that high pressure could effectively facilitate the nuclear fusion of hydrogen isotopes. This conjecture has been studied in a number of theoretical works (see, e.g., the reviews in Refs. 2, 3, and 4). Quantitative estimations of the appropriate pressure were made by Zel'dovich[5] and by Salpeter and Van Horn.[6] For example, it is necessary to compress cold hydrogen by pressure $P > 10^{15}$ bar to density $n > 10^5$ g/cm^3. Such a pressure exists in the bowels of massive stars; however, this method of fusion reaction facilitation is unrealistic under conventional (laboratory or industrial) conditions. It is interesting to consider the origin of such high requirements for pressure and to examine possible ways to reduce these requirements.

The parameter that determines the rate of nuclear fusion is the probability of quantum-mechanical tunneling. This probability is determined by $\exp(-W)$, where

$$W = \frac{2}{\hbar}\int_{R_n}^{R_0} [2M[e\varphi(r) - E]]^{1/2}\, dr \ , \qquad (1)$$

where

M = reduced mass of hydrogen nuclei (deuterium or tritium)

$\varphi(r)$ = potential energy of the Coulomb interaction of the nuclei

E = initial kinetic energy of the relative movement of the nuclei

R_n = radius of the nuclear interactions (it is usually assumed that $R_n = 0$)

R_0 = classical distance of the closest approach of the nuclei.

The determination of W has been the subject of numerous works.[7-14] The analysis takes into account the details of the internuclear potential (determined in the Born-Oppenheimer approximation),[7,8] the many-body effects,[8,10] and the effects of the solid-state environment.[11-14] It was established that the actual value of W is ~100 to 140, whereas a value $W \simeq$ 60 to 70 is necessary to obtain a detectable fusion reaction rate in solids.

It is useful for future reference to estimate the possible values of W. We describe the screening effect by the factor $\exp(-\lambda r)$. Writing the function $\varphi(r)$ in the form $\varphi(r) = e\exp(-\lambda r)/r$, we see that the exponent W is a function of energy E and screening parameter λ. In Fig. 1, we show the level lines of the function $W_0 \equiv W(R_n = 0)$ on the (λ, E) plane. We can conclude that the parameters λ and E are mutually complementary; i.e., we can compensate for the effects of a decrease in E by an increase in λ, and vice versa.

The usual assumption that $R_n = 0$ leads to some increase in the actual value of W. This is because the cross sections of $D + D$ and $T + D$ nuclear interactions increase with decreasing energy. Let us consider this item in detail.

It is quite reasonable to suppose that the matrix elements (in wave functions of a compound nucleus representation) of nuclear scattering amplitude are constants in the limiting case of low energy. Within the framework of this assumption, the effective cross section of a reaction has the form

$$\sigma_{eff} = C \cdot |\psi(0)|^2 / v \ , \qquad (2)$$

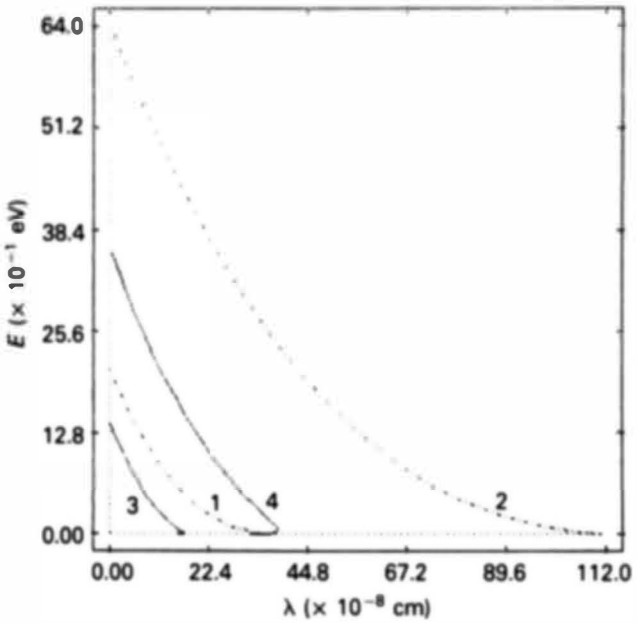

Fig. 1. Level lines of the functions $W_0 = W(R_n = 0)$ (dashed-dotted) and W (solid) on the plane (λ, E) for the T + D reaction. Curves 1 and 3 correspond to $W_0 = W = 70$, and curves 2 and 4 correspond to $W_0 = W = 40$.

where

v = velocity of relative movement

$\psi(0)$ = wave function of nuclear relative movement in the limit $r \to 0$.

Using the definition in Eq. (2), we write

$$|\psi(0)|^2 = W \cdot [\exp(W) - 1]^{-1} \simeq W \exp(-W) \ . \qquad (3)$$

The cross-section measurements of the D + D and D + T reactions in the low-energy range were the subject of numerous research works (see, e.g., Refs. 15 and 16). We can determine the value of C by the use of the data of dependence $\sigma_{eff}(E)$, which are listed in Ref. 16. Arnold et al. examined the constancy (in the 10- to 100-keV energy range) of the value $E \cdot \sigma_{eff}(E) \cdot \exp[W(E)]$. The results of their measurements confirmed this circumstance. The value of C [in Eq. (2)] is $\simeq 2 \times 10^{-16}$ cm^3/s for the D + D reaction and $\simeq 2 \times 10^{-14}$ cm^3/s for the D + T reaction.

It is believed that the C/v ratio is the cross section σ_{nuc} of pure nuclear (without Coulomb effect) interaction. This conforms with general conclusions of the theory of inelastic collisions of slow particles (see, e.g., Ref. 17). The radius R_n of nuclear interactions can be determined by $R_n \simeq (C/\pi \cdot v)^{1/2}$. For example, if $E = 1$ eV, then $v = 1.3 \times 10^6$ cm/s; then, $R_n \simeq 7 \times 10^{-11}$ cm for the T + D reaction. The part of W connected with R_n not being zero can be determined as

$$\delta W \simeq (4 \cdot e/\hbar) \cdot (2 \cdot M \cdot R_n)^{1/2} \ .$$

If $E = 1$ eV, then $\delta W \simeq 30$. The actual value of W is $W_0 - \delta W$. In Fig. 1, we present the level lines of the function $W(\lambda, E)$ on the (λ, E) plane.

Using the results of calculations of function $W(\lambda, E)$, we can determine the value of λ that is required for significant enhancement of the cold fusion rate. A value $\lambda_1 = 2 \times 10^9$ cm^{-1} is necessary for detectable cold ($E = 0$) nuclear fusion in solids. Nuclear fusion in solids can be of practical significance if $\lambda_2 = 4 \times 10^9$ cm^{-1}. If $E = 100$ eV, the corresponding values are $\lambda_1 = 10^8$ cm^{-1} and $\lambda_2 = 2 \times 10^9$ cm^{-1}.

It is interesting to compare these values of λ with the characteristic values of screening parameters in a gas of quasi-free electrons in a metal. Within the Thomas-Fermi (T-F) approximation framework, the screening parameters are determined by

$$\lambda_F = 2em^{1/2}n^{1/6}\hbar^{-1} \simeq 1.3 \times 10^8 \text{ cm}^{-1} \ , \qquad (4)$$

where $n \simeq 10^{22}$ cm^{-3} is the density of the free electrons. The value of λ is approximately ten times lower than the value required. Note also that the screening parameter λ_F increases with an increase in the electron density n. This dependence, however, is very weak ($\lambda \propto n^{1/6}$); to increase the value of λ by ten times, it is necessary to compress a metal sample $>10^6$ times. The latter value is in good agreement with the estimations given in Refs. 5 and 6.

The diamond anvil cell is the most powerful instrument available today for generating static ultrahigh pressures.[18] The combination of cell design, precise workmanship, and gasketing has resulted in devices that can reach pressures beyond 2 to 4 Mbar. The further development of this technique will make pressures of 10 Mbar possible. The pressure of $>10^{11}$ Mbar that is required for the compression of the metal sample is unrealistic under current laboratory or industrial conditions. For the practical realization of the Wildhack idea (high-pressure nuclear fusion), we must find a new physical object with exotic properties (see, e.g., Refs. 19, 20, and 21).

As one of the "pretenders" to this role, we consider a specific defect in the crystalline lattice of some light element hydrides, called the "E-cell." This object was introduced and studied in Refs. 22 through 28. In the E-cell, enhancement of the fusion rate is possible. There are a number of physical phenomena in the E-cell, each of which somewhat decreases the W value, and the whole complex of these phenomena reduces the pressure requirements needed for the enhancement of the fusion rate. The resulting pressure requirements are within the limits of the possibilities of modern techniques.

The idea and the formation of the E-cell are clarified in Sec. II, where the main phenomena developed in the E-cell after its formation are considered qualitatively. To begin with, we use simple models in Sec. II. In the following sections, we use stricter models for the quantitative estimations. In Sec. III, we describe the general picture of the evolution of the E-cell. We determine the variations of the energy, volume, and structure parameters of the E-cell. The dynamics of the hydrogen nuclei in the E-cell is investigated in Sec. IV. We use the idea of a pseudoparticle with nonisotropical mass, which moves in an effective potential hole of the E-cell. Some characteristics of this motion correspond to the characteristics of the motion of real hydrogen nuclei in the E-cell. In Sec. V, we determine the screening effects of the electron subsystem of the E-cell. In Sec. VI, it is shown that the eventual result of the combined action of the main phenomena in the E-cell is a significant enhancement of the fusion rate. The conditions under which cold fusion in solids results in a detectable neutron yield can be created by the use of modern techniques. The concluding remarks (Sec. VII) contain some considerations about the direction of future investigations.

In this technical note, we use the Hartree system of atomic units. In this system, the length scale is defined as $a \equiv \hbar^2/e^2m \simeq 0.529$ Å $= 5.29 \times 10^{-9}$ cm. The energy scale

E_0 is equal to $e^2/a \simeq 4.36 \times 10^{-11}$ ergs = 27.2 eV. The density scale N_0 is $a^{-3} \simeq 6.75 \times 10^{24}$ cm^{-3}, and the pressure scale P_0 is $E_0/4\pi a^3 \simeq 2.34 \times 10^{13}$ din/cm^2 = 23.4 Mbar. In these units, the space variable is $x = r/a$, and the energy, density, and pressure variables are $\mathcal{E} = E/E_0$, $\mathfrak{N} = n/N_0$, and $\mathfrak{P} = P/P_0$, respectively.

II. THE E-CELL: FORMATION, STRUCTURE, AND MODELS

The E-cell[22] is a radiation defect in crystalline lattice hydrides A_xH_y (x and y are determined by the chemical formula of the hydride), where A is one of the isotopes: ^{3}He, ^{6}Li, ^{7}Be, or ^{10}B. An E-cell forms as a result of the capture of a thermal neutron by the nucleus of an atom A in one of the following reactions:

$$^3\text{He} + n \rightarrow \text{T} + p + 0.746 \text{ MeV} ,$$

$$^6\text{Li} + n \rightarrow {}^4\text{He} + \text{T} + 4.785 \text{ MeV} ,$$

$$^7\text{Be} + n \rightarrow {}^7\text{Li} + p + 1.650 \text{ MeV} ,$$

or

$$^{10}\text{B} + n \rightarrow {}^7\text{Li} + {}^4\text{He} + 2.791 \text{ MeV} .$$

The reaction products leave the cell in 10^{-17} s, which is much shorter than the reconstruction time of the electron system ($\sim 10^{-15}$ to 10^{-12} s), and initially, the E-cell has a surplus of electrons, which form the electronic shell of an atom A. The problem of the confinement of surplus electrons is discussed in Sec. II.B, as well as in Refs. 22 through 25.

Now we define the geometry of the E-cell. We consider, for definition, the face-centered cubic crystalline structure of a NaCl-type lattice (LiH has such a structure[29]). This consideration is not correct for BeH_2 hydride. The BeH_2 lattice has a hexagonal structure. The ^{7}Be isotope is unstable; therefore, the investigation of the BeH_2 hydride is of no practical interest. As for boron, it is well-known that boron forms several stable hydrides (e.g., B_2H_6, B_4H_{10}, etc.); however, their crystalline structure is still unknown. Helium hydride does not exist under normal conditions. There is no doubt that the H + He mixture forms a hydride under high pressure, but its crystalline structure is unknown. Thus, the results of the following considerations should be regarded as tentative for the boron and helium hydrides.

II.A. The E-Cell Structure

Let us define that the center of the E-cell is located at the site of the fission nucleus, and the centers of the neighboring metal atoms are connected by straight lines. The border of the E-cell formed by these lines is an octahedron (see Fig. 2). Six hydrogen nuclei together with both their own electrons plus the Z electrons that earlier formed the electron shells of the central atom A are located inside the E-cell.

It is practically impossible strictly to investigate a system consisting of 24 nuclei and $N = 18Z + 6$ (or more) electrons. Therefore, we consider several models of the E-cell, each of which describes one of the E-cell phenomena.

One of these models is the so-called "shell model" of the E-cell (see Refs. 22 and 27). It is the analog of the Wigner-Seitz approximation for a separate atom. Within the shell model framework, we replace the boundary octahedron by a sphere with the same volume. The radius R_c of this sphere is related to the crystalline lattice constant L by $R_c = L \cdot \pi^{-1/3}$. Using the considerations of Evjen (see, e.g., Ref. 30) regarding the charge distribution between the cells of a crystalline lattice, we infer that one-fourth of all nuclei placed on the octahedron's edges and one-sixth of all nuclei placed in the octahedron vertices should be attributed to the nuclear system of the E-cell. The corresponding atomic electrons should be attributed to the electron system of the E-cell. Thus, we must attribute to the boundary of the E-cell the positive charge of four atom A nuclei. We assume that this charge is uniformly distributed along the sphere's surface, while the charge of N_e electrons is continuously distributed in the E-cell volume. The total number of electrons in the E-cell N_e is equal to $5Z + 6$ before and immediately after the E-cell formation. This number is equal to $4Z + 6$ long after the E-cell formation, when the surplus electrons leave the E-cell. We use the shell model in Sec. III to investigate the evolution of the E-cell.

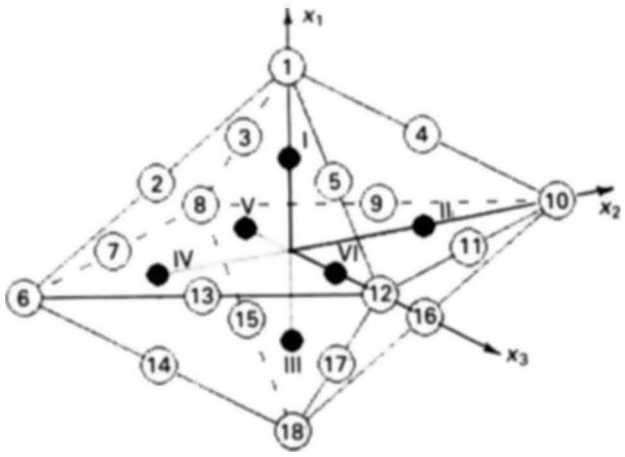

Fig. 2. Geometry of the E-cell with the Cartesian coordinate system. The open circles are the lithium atoms, and the closed circles are the hydrogen atoms.

Now we determine the qualitative characteristics of the processes that develop in the E-cell. In this section, we use simple models to obtain the obvious results. In the following sections (see also Refs. 22 through 28), we use stricter models for the quantitative description of the E-cell phenomena.

II.B. Trapped Electrons in the E-Cell

Let us consider the confinement of the surplus electrons in the E-cell. A naive estimate using the ratio R_c/v (where $v \simeq 10^8$ cm/s is the electron velocity) gives the stay time of electrons in the E-cell, $T \simeq 10^{-12}$ s. There is a possibility of increasing the time by using some features of electron/atom interaction in a defect cell. This assumption stems from numerous experimental results on trapped electrons in crystalline media (see, e.g., the review in Ref. 31). An analogous estimation for thermal electrons gives $T \simeq 10^{-11}$ s. In fact, the average existence of the trapped electrons in a defect cell is several microseconds. Some theoretical models have been applied to explain the stability of trapped electrons.[32-34] The electron is assumed to be located at the center of a spherical cavity, and it interacts with the surrounding atoms. The variation method was applied to the total energy E_t of the system to obtain the minimum energy. Some amount of energy would be expended when the electron leaves the cavity. This is because when the electron leaves the cell, it attaches to one of the boundary atoms. The transformation of this atom into a negative ion is accompanied by an increase in the total energy E_t of the system. The difference in total energy between

the initial (the electron in the cell) and the intervening (the electron attached to a boundary atom) states can be interpreted as the height $[E]$ of the potential barrier for a surplus electron in the cell. The calculations are detailed in Refs. 32, 33, and 34. The results of this approach generally explain the experimental facts quite well.

For our purposes, we can estimate a value of $[E]$ for a LiH crystal by using the T-F model (see Refs. 35, 36, and 37 and Appendix A) for the description of lithium atoms (total energy is E_a) and negative ions Li^- (total energy is E_i), which have a size R_0 in a crystal. In accordance with data listed in Ref. 29, $R_0 \simeq 1.5$ Å under normal conditions. The height of the potential barrier $[E] \simeq 6$ eV in this case. For boron [$R_0 \simeq 0.9$ Å (Ref. 29)], the corresponding result is $[E] \simeq 11$ eV. To solve the problem of confinement of the surplus electrons in the E-cell, we must compare the value of $[E]$ with the average energy $\langle E \rangle \simeq 16Z^{4/3}$ eV of electrons that remain in the E-cell after the fission of a central nucleus. We see that the value of $[E]$ is small for the confinement of the surplus electrons in the E-cell in the crystal under normal conditions. For instance, for lithium, $\langle E \rangle \simeq 60$ eV; for boron, $\langle E \rangle \simeq 140$ eV.

To confine the surplus electrons in the E-cell, we must rely on the fact that the value of $[E]$ increases with pressure P in a crystal. We demonstrate this by the following method. Let us determine the values of E_a and E_i for atoms and negative ions compressed to size R_0 (which corresponds to size $X_0 = R_0/a$ in Hartree units). Simultaneously, we determine the pressure needed for this compression. Considering X_0 as a variable parameter, we immediately derive the dependence of $[E] = E_i - E_a$ on pressure P. The results of these calculations are shown in Table I. We see that to confine the surplus electrons in the E-cell, the pressure in the LiH crystal must be >40 to 50 Mbar. For boron, this value is 300 to 400 Mbar.

Of course, we must consider these results as estimations only. They show a general tendency – the height of the barrier $[E]$ increases with an increase in pressure P. A special, more careful consideration is needed to quantitatively determine the pressure needed for the confinement of the surplus electrons in the E-cell.

II.C. Simple Model of the Electrical Potential Distribution

Let us consider the possible shape of the electrical potential distribution in the E-cell. The total potential φ is the sum of the potentials φ_e created by the electrons and φ_n created by the nuclei. We calculate these potentials within the framework of the shell model of the E-cell.

We assume that the electrons are distributed uniformly in the E-cell volume, and the hydrogen nuclei are initially placed on the boundary sphere. The electron density is $n = 3N_e/4\pi R_c^3$.

Before the E-cell formation, the potentials φ_e and φ_n are equal:

$$\varphi_e \simeq -2\pi e N_e (R^2 - r^2/3)$$

and

$$\varphi_n = Ze/r + (4Z + 6)e/R_c \ .$$

The total potential ($\rho \equiv r/R_c$) is

$$\varphi = (e/2R_c) \cdot [2Z/\rho - (7Z + 6) + (5Z + 6)\rho^2] \ .$$

The dependence of φ on ρ (for $Z = 3$) is depicted by curve 1 of Fig. 3.

Immediately after the E-cell formation, the total potential is

$$\varphi = (e/2R_c) \cdot [-(7Z + 6) + (5Z + 6)\rho^2] \ .$$

This dependence is depicted by curve 2 of Fig. 3. We see that close to the E-cell boundary, a change in potential creates an electrical field that draws the positively charged hydrogen nuclei to the center of the E-cell.

Let us suppose that one of the hydrogen nuclei is displaced into the center of the E-cell. Then, the total potential is

$$\varphi = (e/2R_c) \cdot [2/\rho - (7Z + 6) + (5Z + 6)\rho^2] \ .$$

This dependence is depicted by curve 3 of Fig. 3.

If the surplus electrons leave the E-cell, the total potential is

$$\varphi = (e/R_c) \cdot [1/\rho - 2(Z + 2) + (2Z + 3)\rho^2] \ .$$

This dependence is depicted by curve 4 of Fig. 3.

By analyzing the depicted results, we can draw the following conclusions:

1. The screening of the electrical field of the positive charge placed at the E-cell center is described by the specific expression

$$\varphi(r) = (e/r) \cdot (1 - r/R_0) \ ,$$

where we assume $r \ll R_c$.

TABLE I

Energy Characteristics of Neutral Atoms and Negative Ions Compressed by Pressure P in the Megabar Range

		$Z = 3$				$Z = 5$			
X	R (Å)	P (Mbar)	E_a (eV)	E_i (eV)	$[E]$ (eV)	P (Mbar)	E_a (eV)	E_i (eV)	$[E]$ (eV)
1.0	0.53	143.0	−267	−180	87.1	307.0	−893	−783	110.0
1.2	0.64	46.7	−289	−232	56.8	98.6	−941	−869	70.7
1.4	0.74	17.3	−300	−261	39.2	36.2	−963	−916	48.1
1.6	0.85	6.98	−306	−278	28.3	14.6	−976	−942	34.4
1.8	0.95	3.00	−309	−288	21.1	6.32	−982	−958	25.1
2.0	1.06	1.33	−311	−294	16.2	2.88	−986	−967	19.1
2.2	1.16	0.46	−313	−302	11.1	1.35	−988	−972	15.6

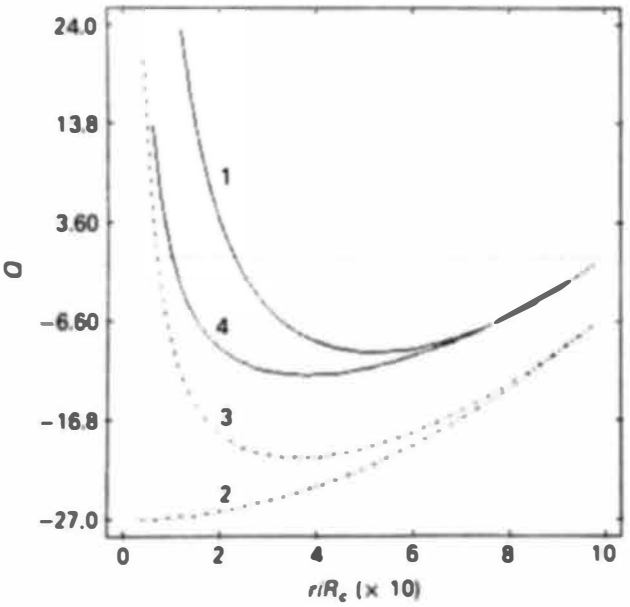

Fig. 3. Potential distributions in the E-cell at different stages of E-cell evolution (the model of a uniform electron density). Curves 1 and 4 show potential distributions in the neutral E-cell (curve 1 corresponds to the cell before fission of the central nucleus, and curve 4 corresponds to the last stages of E-cell evolution). Curves 2 and 3 correspond to the charged E-cell (curve 2 corresponds to the E-cell immediately after the E-cell formation, and curve 3 corresponds to the E-cell after the displacement of a hydrogen nucleus into the center).

2. Within the framework of these assumptions, the screening length R_0 is determined by $R_0 = R_c/Z_{eff}$, where $Z_{eff} = (7Z + 8)/2$ if the surplus electrons are confined in the E-cell and $Z_{eff} = 2(Z + 2)$ if the surplus electrons leave the E-cell.

3. The screening length R_0 in the E-cell depends on the electron density more strongly ($R_0 \propto n^{-1/3}$) than the screening length within the Fermi approximation [see Eq. (4)].

These results were obtained by assuming a uniform distribution of the electron density in the E-cell. These results are very important. In the following, they are defined more accurately by various methods (see Secs. IV and V).

II.D. Dynamic Effects in a Compressed Cell

The quick transformation of a normal cell of a crystalline lattice into an E-cell is accompanied by some dynamic effects that strongly reduce the distances between the hydrogen nuclei. We explain this assertion by the next example.

Let us consider a simple model of a linear crystal that consists of four nuclei. Each of the two middle nuclei has an electrical charge e; each of the two outer nuclei has charge Ze. Some force F compresses the crystal to size D by acting on the boundary nuclei. We assume that the distance between the middle nuclei is d. The potential energy (in appropriate units) of this system $U(D,d)$ is

$$U(D,d) = 8ZD/(D^2 - d^2) + Z^2/D + 1/d + FD \ . \quad (5)$$

The requirement to minimize U gives us the following expressions for equilibrium values D_{eq} and d_{eq}:

$$D_{eq} = Y_{eq} \cdot F^{1/2} \quad \text{and} \quad d_{eq} = y_{eq} \cdot F^{1/2} \ .$$

The values of Y_{eq} and y_{eq} are given in Table II.

Let us assume that our crystal was formed from a crystal of five nuclei that was transformed by the fast removal of the central nucleus (with an electrical charge Ze). In the five-nuclei crystal, the initial equilibrium values of D and d are

$$D_{in} = Y_{in} \cdot F^{1/2} \quad \text{and} \quad d_{in} = y_{in} \cdot F^{1/2} \ . \quad (6)$$

The values of Y_{in} and y_{in} are given in Table II.

After removal of the central nucleus, D_{in} and d_{in} characterize the initial positions of the nuclei in the four-nuclei crystal. The initial nuclear potential energy U_{in} is determined by Eq. (5), where $D = D_{in}$ and $d = d_{in}$. We define $U_{in} = A(Z)F^{1/2}$. The values of A are given in Table II.

After the formation of the four-nuclei crystal, the nuclei start moving from the initial position [Eq. (6)]. The condition $U(D,d) = U_{in}$ determines the curve $d = d(D)$ that bounds the area available for moving. The function $d(D)$ has a minimum, which is determined by $d_{min} = y_{min}F^{1/2}$. The values of y_{min} are given in Table II. The value of d_{min} determines the minimal distance between the two middle nuclei. The d_{eq}/d_{min} ratio (see Table II) does not depend on force F and can be considered as a universal measure of the gain resulting from the dynamic effects. According to the data in Table II, we can strongly (by two to eight times) reduce the internuclear separation by using the dynamic effects.

Recall that the transformation of a normal cell of a crystalline lattice into an E-cell is the result of neutron capture by the nucleus of an atom of metal. The reaction products leave the cell in $\simeq 10^{-17}$ s, which is much shorter than the period of the oscillations of the nucleus in a crystalline lattice; therefore, the fast removal of a nucleus is performed.

II.E. Qualitative Conclusions

The combination of the results of a consideration of separate phenomena in the E-cell allows us to draw a number of qualitative conclusions:

1. Immediately after the transformation of a normal cell of a crystalline lattice into an E-cell, the free-electron density in this cell increases.

2. If a crystal is compressed by a pressure P that is in the megabar range, a potential barrier exists on the boundary of the E-cell that confines the surplus electrons inside the E-cell. The efficiency of the confinement of the surplus electrons increases with the increase of the pressure in a crystal.

TABLE II

Values of Various Parameters

Z	Y_{eq}	y_{eq}	Y_{in}	y_{in}	A	y_{min}	d_{eq}/d_{min}
1	3.6	1.3	4.9	2.5	7.7	0.63	2.07
2	5.0	1.5	7.6	3.9	11.0	0.45	3.32
3	6.2	1.6	10.0	5.2	14.0	0.35	4.70
4	7.4	1.8	12.0	6.4	17.0	0.29	6.21
5	8.5	1.9	15.0	7.6	20.0	0.24	7.87

3. The screening of the Coulomb potential of a positive charge in the E-cell differs from the usual screening both by the space distribution of the potential and by the dependence of parameters of screening on the electron density.

4. The dynamic effects, accompanied by the quick transformation of a normal cell of a crystalline lattice into an E-cell, create conditions for a strong reduction of the internuclear separation.

Let us give a more precise definition of these qualitative assertions. We must investigate more realistic models. This investigation would allow us to obtain quantitative estimations of the effects and (what is more important) to determine methods to intensify these effects. It is possible to reduce the pressure requirements needed to enhance the fusion rate through these investigations.

III. GENERAL PICTURE OF THE EVOLUTION OF THE E-CELL: SIZE, STRUCTURE, AND ENERGY VARIATIONS

It is complicated to make a general investigation of the electron-nuclear system of an E-cell. The problem may be simplified by setting limited goals such as the following:

1. estimation of the energy characteristics of the process that accompanies the evolution of the E-cell
2. determination of the character and directions of changes to the size of the E-cell
3. estimation of the possibility of various configurations of the hydrogen atoms in the E-cell.

We can use the shell model (see Sec. II.A) of the E-cell within the T-F approximation framework (see Appendix A). The main judgments on the processes of E-cell evolution are based on investigations of the energy variations. We assume that the direction of the changes in the E-cell parameters is determined by the requirements to minimize the total energy of the electron-nuclear system (see also Refs. 25 and 27). The basic equations for the determination of the energy variations are given in Appendix A.

We assume that the electrical charge of hydrogen nuclei is uniformly distributed along the surface of an inner sphere of radius R_s ($X_s = R_s/a$ in Hartree units). We use the following designations: the electrical charge at the center of the E-cell is Z_0 (in Hartree units); at the inner shell, it is Z_s; and at the boundary sphere, it is Z_c. The total number N_e of electrons in the E-cell is equal to $5Z + 6$ before and immediately after the E-cell formation, and it is equal to $4Z + 6$ much longer after the E-cell formation, when the surplus electrons leave the E-cell. The value of Z_s is equal to 6 before and immediately after the E-cell formation. Later on, the displacement of some of the hydrogen nuclei into the E-cell center is possible. The total charge dZ of the E-cell is equal to $(Z_0 + Z_s + Z_c) - N_e$. We consider sets of parameters Z_0, Z_s, and N_e that are of the most interest in our investigations. These sets are listed in Table III.

TABLE III

Charges in the Various Parts of the E-Cell at Different Stages of E-Cell Evolution

Z_0	Z_s	N_e	Stage of E-Cell Evolution
Z	6	$5Z + 6$	Before central nucleus fission
0	6	$5Z + 6$	Immediately after E-cell formation
1	5	$5Z + 6$	After the displacement of one or two hydrogen nuclei into the center; surplus electrons are in the E-cell.
2	4	$5Z + 6$	
1	5	$4Z + 6$	After the displacement of hydrogen nuclei into the center; surplus electrons leave the E-cell.
2	4	$4Z + 6$	

III.A. Compressibility of the E-Cell

Let us consider, for example, the E-cell before the fission of the central nucleus. The total energy of the electron-nuclear system of the E-cell is a function of the following parameters: the cell radius X_c, the radius of the inner hydrogen shell X_s, and the nuclear charge of the metal atoms Z (all parameters are in Hartree units). The energy varies if we vary the radius X_s (both X_c and Z are constant). For example, at $X_c = 5$ and $Z = 3$, the value of total energy is minimal if $X_s = 3.9$. We can assume that this value of X_s determines the equilibrium position of the inner hydrogen shell in a normal cell of the crystalline LiH lattice. The corresponding value of E_{tot} is $\simeq -168$ eV. The pressure that is needed to compress a cell to size X_c varies with X_s in the same manner as the energy. If $X_s = 3.9$, then $P \simeq 2.24$ Mbar. These data describe the equilibrium cell with the chosen parameters Z and X_c. For different X_s values, the corresponding values of $E_t = \min[E_{tot}(X_s)]$ and pressure P are listed in Table IV (we assume $Z = 3$).

Note that the pressure needed to compress a cell to size X_c is near the pressure P_e needed to confine N_e electrons inside a sphere with radius X_c. The values of P_e are determined by Eq. (A.9), and they are also shown in Table IV. The data in Table IV show that $P < 1$ Mbar (in Hartree units, $\Psi < 0.04$) if $X_c > 6$. The value of $\Psi \simeq 0.04$ is within the accuracy range of our calculations. We may assume that $X_c = 6$ ($R_c = 3.2$ Å) characterizes a compressed cell in a crystalline LiH lattice. The crystalline lattice constant L (coupled with R_c by $L = R_c \pi^{1/3}$, see Sec. II.A) is equal to 4.5 Å if $R_c = 3.2$ Å. This value of L is near the actual value of the crystalline lattice constant, $L = 4.1$ Å, for LiH (Ref. 29).

TABLE IV

Total Energy of the E-Cell Under Pressure P in the Megabar Range

X	R_c (Å)	P (Mbar)	P_e (Mbar)	E_t (eV)
3.0	1.59	27.9	26.4	55.4
3.5	1.85	12.8	11.6	−44.2
4.0	2.12	6.57	5.65	−104.0
4.5	2.38	3.69	2.97	−143.0
5.0	2.65	2.24	1.65	−168.0
5.5	2.91	1.44	0.96	−185.0
6.0	3.17	0.98	0.58	−197.0
6.5	3.44	0.68	0.36	−205.0

The value of X_c decreases if pressure P in the crystal increases. For example, according to Table IV, to compress a cell to a size $X_c = 4.0$, a pressure $P \simeq 6.6$ Mbar is necessary. Let us note that the results in Table IV are in good agreement with the results of calculations of the sizes of separate atoms, given in Sec. II.B. Indeed, the size of the E-cell L_c (determined in conformity with the definition of the E-cell: it is the distance from the center to an angular point of the octahedron) is equal to the crystalline lattice constant L in a cubic lattice. We can determine the value of L_c by the obvious equation, $L_c = 2 \cdot [R_a(Z) + R_a(Z = 1)]$. According to the data collected in Table I, the value of $R_a(Z = 3)$ is equal to 0.85 Å if $P = 7$ Mbar. Supposing that $R_a(Z = 1) = 0.5$ Å, we conclude that $L_c = 2.7$ Å; correspondingly, $R_c = 1.85$ Å and $X_c = 3.5$. The latter is close to the $X_c = 4$ that is cited in Table IV.

III.B. Energy Characteristics of the E-Cell Evolution

Let us consider the structure of the E-cell immediately after its formation. If we assume that electrons are confined in the E-cell, we should choose the following set of parameters: $Z_0 = 0$, $Z_s = 6$, and $dZ = Z$. In this case, as well as in one considered earlier, there is an equilibrium radius X_s of the inner hydrogen shell. The corresponding values of $E_t = \min[E_{tot}(X_s)]$ and pressure P on the boundary of the E-cell are given in Table V for various values of the E-cell radius X_c.

Let us compare these results with the data given in Table IV. We see that the removal of the central nucleus causes an increase in pressure P on the boundary of the E-cell. In other words, the E-cell starts to dilate immediately after its formation. It is important to note that the removal of the central nucleus causes an increase in the total energy of the electron-nuclear system of the E-cell. The value δE of this increase is $\simeq$200 eV, which is close to the total energy of the electron shells of the destroyed central atom. It is quite natural that the destruction of the central atom leads to an energy transfer from the electron shell to the electron-nuclear system of the E-cell. Let us also note that the equilibrium radius of the inner hydrogen shell decreases in comparison with that in a normal cell. In other words, the displacement of the hydrogen nuclei to the center of the E-cell leads to an energy gain in the electron-nuclear system of the E-cell. This gain increases if one of the hydrogen nuclei transfers to the center of the E-cell. This situation is described by the following set of parameters: $Z_0 = 1$, $Z_s = 5$, and $dZ = Z$. The corresponding results are listed in Table V. We see that such a reconstruction of the inner structure of the E-cell also leads to an energy gain. The value of this gain is 30 to 40 eV (depending on the pressure in the crystal). We may suppose that the energy gain transforms to the kinetic energy of the hydrogen nuclei.

The same effect (a decrease in the total energy of the electron-nuclear system of the E-cell) accompanies the displacement of the following hydrogen nucleus to the center. This situation is described by the following set of parameters: $Z_0 = 2$, $Z_s = 4$, and $dZ = Z$. The results are given in Table V.

If surplus electrons leave the E-cell, the pressure and the total energy of the electron-nuclear system of the E-cell decrease. The corresponding results are collected in Table VI. Note that the movements of hydrogen nuclei inside the neutral ($dZ = 0$) E-cell lead to a pressure decrease to values smaller than the initial ones. This means that the E-cell reduces to a fraction of its former size. The volume of the E-cell can be reduced by half of its initial value.

III.C. Some Results

The results of our consideration allow us to come to the following conclusions:

1. We can estimate the size of a normal cell as the sum of the sizes of atoms that form the crystal.

2. The pressure P needed to compress the E-cell to a size R_c is near the pressure P_e in a degenerated electron gas of density $n = 3N_e/4\pi R_c^3$. The values of P and P_e vary proportionally to each other when the E-cell size varies.

3. Immediately after the transformation of a normal cell of a crystalline lattice into an E-cell, the pressure on its boundary increases by half of the initial value, and the total energy of the electron-nuclear system also increases. The value of this increase is near the value of the total energy of the electron shells of the destroyed central atom.

4. After the formation of the E-cell, hydrogen nuclei start moving to the E-cell center. The displacement of hydrogen

TABLE V

Energy Characteristics of the E-Cell in LiH at Different Stages of E-Cell Evolution When the Surplus Electrons Remain in the E-Cell

		$Z_0 = 0$		$Z_0 = 1$		$Z_0 = 2$	
X	R (Å)	P (Mbar)	E_t (eV)	P (Mbar)	E_t (eV)	P (Mbar)	E_t (eV)
3.0	1.59	32.4	441.6	31.5	400.9	30.9	303.1
3.5	1.85	14.8	309.0	14.4	272.9	14.2	181.5
4.0	2.12	7.50	224.5	7.26	191.7	7.22	104.7
4.5	2.38	4.09	167.0	3.97	136.8	3.85	53.74
5.0	2.65	2.39	126.9	2.31	98.28	2.17	18.17
5.5	2.91	1.46	97.37	1.41	70.58	1.38	−7.38
6.0	3.17	0.95	66.68	0.90	49.77	0.87	−26.1
6.5	3.44	0.69	47.01	0.60	33.99	0.56	−40.3

TABLE VI

Energy Characteristics of the E-Cell in LiH at Different Stages of E-Cell Evolution After the Surplus Electrons Have Left the E-Cell

		$Z_0 = 0$		$Z_0 = 1$		$Z_0 = 2$	
X	R (Å)	P (Mbar)	E_t (eV)	P (Mbar)	E_t (eV)	P (Mbar)	E_t (eV)
3.0	1.59	23.2	287.1	22.4	247.3	21.9	150.8
3.5	1.85	10.4	192.8	10.0	157.5	9.89	67.0
4.0	2.12	5.22	133.7	5.01	101.5	4.98	15.2
4.5	2.38	2.81	94.01	2.69	64.20	2.54	−18.3
5.0	2.65	1.62	66.78	1.54	38.56	1.51	−41.2
5.5	2.91	0.97	47.01	0.93	20.51	0.89	−57.1
6.0	3.17	0.71	33.88	0.59	7.195	0.55	−68.5
6.5	3.44	0.51	17.01	0.38	−2.67	0.34	−76.7

nuclei is accompanied by an energy gain of tens of electron volts per nucleus. This energy transforms into the kinetic energy of the hydrogen nucleus movement.

5. If surplus electrons leave the E-cell, the volume of the E-cell may be reduced by half of its initial value.

These are the main features of the E-cell evolution process.

IV. HYDROGEN NUCLEAR DYNAMICS IN THE E-CELL: THE DISCRETE MODEL

One of the problems we face in investigating the E-cell is the description of the interaction of the compressed atoms. We should choose a pairwise interaction from among a great many interacting atoms. This problem is not yet solved rigorously within the framework of many-body theory. Therefore, we confine ourselves to an approximation where only pairwise interactions are taken into account.

Let us choose a pair of interacting atoms in our system. The other atoms of the system compress each atom of the chosen pair. The key idea is to model this effect by considering this pair of atoms in a free-electron gas of density n determined by pressure P in the crystal according to Eq. (A.9). Within the framework of this approximation, each atom of the chosen pair is compressed by the pressure of electrons, which imitate the influence of the rest of the atoms of the initial system.

Thus, we reduce the problem of describing the interaction between a number of squeezed atoms in the crystal to the problem of describing the pairwise interaction of atoms in the free-electron gas. It is important to note that the proposed model reflects the real situation in the E-cell, in which the pressure is a result of the collective action of all electrons (see Sec. III.A).

IV.A. Atoms in a Free-Electron Background

It is interesting for subsequent consideration to determine the total energy E_t of atoms that are in the electron gas. The value of E_t is determined by the integral in Eq. (A.12). The results for the various elements are given in Table VII. We see that the total energy E_t of atoms increases with an increase in the electron pressure P. This dependence is weak; e.g., if pressure varies 30 times (correspondingly, the density varies 10 times), the total energy varies less than one-tenth of its value. The reason for this is the weak dependence of the inner atomic structure on the external conditions, just as energy (both potential and kinetic) is mainly connected with the inner electrons.

Let us compare the data in Table VII with the results of calculations of the total energy of separated atoms in Sec. II.B (see Table I). We see that the absolute values of E_t in Table VII are lower than those in Table I, but the variations of E_t are the same within the framework of both models.

TABLE VII

Total Energy (eV) of Atoms in a Free-Electron Background with Density $\mathfrak{N}$ Under Pressure P

	P (Mbar)				
	1.0	3.0	5.0	10.0	30.0
	$\mathfrak{N}$				
	0.031	0.056	0.073	0.100	0.200
$Z = 1$	−22.47	−21.81	−21.31	−20.39	−17.82
2	−96.96	−95.86	−95.22	−93.54	−89.17
3	−231.9	−230.6	−229.5	−227.3	−221.4
4	−432.7	−431.3	−429.8	−427.3	−420.1
5	−703.9	−702.2	−700.5	−697.7	−689.6
6	−1049.0	−1047.0	−1045.0	−1042.0	−1032.0

IV.B. Atomic Interaction in the E-Cell

Let us consider the problem of the pairwise interaction of two atoms of nuclear charges Z_1 and Z_2 that are in the free-electron gas. We can neglect the comparatively weak quantum effects that are responsible for binding atoms into a molecule, because the E-cell phenomena start when the distances between nuclei become smaller than the atomic size.

In this case, the interaction is determined by the Coulomb repulsion of the nuclei and the variations of the total energy of the electron system. To determine the latter, one should first solve the equation for the electrical potential $\varphi(\boldsymbol{r})$:

$$\Delta\varphi = 4\pi e[n - n_0 - Z_1\delta(\boldsymbol{r} - \boldsymbol{r}_1) - Z_2\delta(\boldsymbol{r} - \boldsymbol{r}_2)] \ . \quad (7)$$

The electron density n is related to the potential φ by

$$3\pi^2\hbar^3 n = \{p_1 + [2me(\varphi - \varphi_0)]^{1/2}\}^3 \ ,$$

where

$$p_1 = me^2/\pi\hbar \ ,$$

$$\varphi_0 = (p_0 - p_1)^2/2me \ ,$$

and

$$p_0 = (3\pi^2\hbar^3 n_0)^{1/3} \ .$$

After $\varphi(\boldsymbol{r})$ and $n(\boldsymbol{r})$ are determined, one should calculate the total energy of the electrons by using Eq. (A.12), in which

$$\varphi_n = eZ_1/|\boldsymbol{r} - \boldsymbol{r}_1| + eZ_2/|\boldsymbol{r} - \boldsymbol{r}_2| \ , \quad (8)$$

The sum

$$U(Z_1, Z_2; r) = E_t(Z_1, Z_2; r) + e^2 Z_1 Z_2/r \ , \quad (9)$$

where $E_t(Z_1, Z_2; r)$ is the total energy of the electron system of two atoms with nuclear charges Z_1 and Z_2 separated by distance r, determines the total energy of the electron-nuclear system. The latter varies with variations of the internuclear distance r. Equation (9) plays the role of the effective potential of the pairwise interaction of the chosen atoms in the E-cell.

This is a very complicated method. The main difficulty of this method is connected with the necessity of integrating a nonlinear two-dimensional elliptical equation, Eq. (7). This problem is solved numerically. An example of the results is given in Fig. 4. We see the equipotential lines of the electrical potential of two atoms with nuclear charges $Z_1 = 1$ and $Z_2 = 3$ separated by distance $X = 1$. The pressure of the electron gas is 10 Mbar. In this case, the total energy of the electron systems of the two atoms is approximately −325 eV.

Having chosen parameters Z_1, Z_2, and P, we can determine the dependence of U on X by this method. However, the use of this method requires long calculations, and it is thus

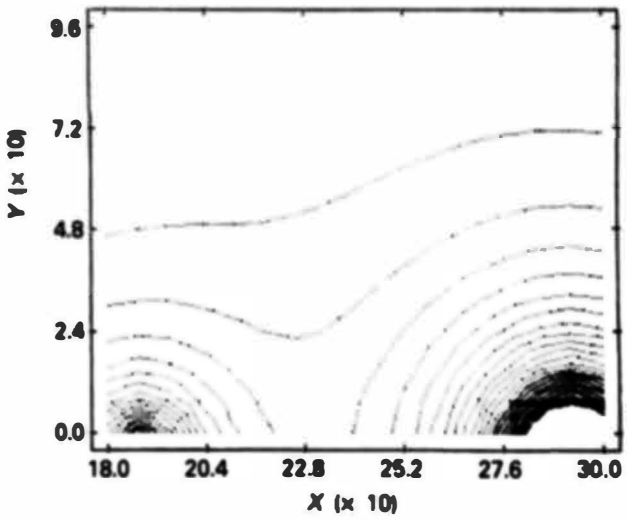

Fig. 4. Equipotential lines of the electrical field near the two atoms (hydrogen and lithium), spaced $X = 1$ apart, in the electron background with electron density $\eta = 0.1$. The electron density and the pressure of the electron gas ($P = 10$ Mbar) correspond to the ones of interest in the E-cell investigations.

inconvenient for the investigation of the nuclear dynamics in the E-cell. For our purposes, it is necessary to find a more operative approximate method. We use an interpolation of the dependence of U on r.

Several conditions determine the form of the functional dependence of U on r. The total energy of the electron system of two atoms with nuclear charges Z_1 and Z_2 separated by distance r is $E_t(Z_1, Z_2; r)$. Two values of this function are known from the results of the investigation of one atom in the electron gas (see Sec. IV.A). These are

$$E_0 \equiv E_t(Z_1, Z_2; r = 0) = E_a(Z_1 + Z_2)$$

and

$$E_\infty \equiv E_t(Z_1, Z_2; r \to \infty) = E_a(Z_1) + E_a(Z_2) \ .$$

When r increases, the value of $E_t(Z_1, Z_2; r)$ decreases from E_0 to E_∞. If $r \gg R_a$, this decrease goes according to the rule $E_t \propto Z_1 Z_2 / r$ because of the last term in the integrand, Eq. (A.12). If $r \simeq R_a$, the results of numerical calculations are in good agreement with the interpolation:

$$E_t(Z_1, Z_2; r) \simeq E_\infty + Q[1 - \exp(-\lambda r)] \ .$$

The condition $E_t(Z_1, Z_2; r \to 0) \to E_0$ determines the value of Q:

$$Q = (E_0 - E_\infty)/\lambda \ .$$

Since the total energy of interaction $U(r)$ [see Eq. (9)] must decrease (when r increases) faster than $1/r$, it determines the value of λ:

$$\lambda = (E_0 - E_\infty)/Z_1 Z_2 e^2 \ . \qquad (10)$$

The values of E_0 and E_∞ are given in Table VII. The resulting values of the effective screening parameters ($S = \lambda a$ in Hartree units) are given in Table VIII. They correspond to the interaction of the hydrogen atom with the atoms of elements of ordering number Z. The resulting dependence of interaction energy U on distance r has the form

$$U(Z_1, Z_2; r) = Z_1 Z_2 e^2 \exp(-\lambda r)/r \ , \qquad (11)$$

where λ is determined by Eq. (10).

TABLE VIII

Effective Screening Parameter S for the Interaction of the Hydrogen Atom with Atoms of Elements of Ordering Number Z

	P (Mbar)				
	1.0	3.0	5.0	10.0	30.0
	$\mathfrak{N}$				
	0.031	0.056	0.073	0.100	0.200
$Z = 1$	1.91	1.92	1.92	1.94	1.96
3	2.19	2.19	2.19	2.20	2.22
5	2.37	2.37	2.38	2.38	2.39

IV.C. Description of the Hydrogen Nuclear Dynamics

Let us consider the dynamics of hydrogen nuclei in the E-cell, taking into account only the pairwise interaction that is described by the interpolating formula, Eq. (11). As in Secs. II and III, we examine the E-cell in a cubic crystalline structure of an NaCl-type lattice. Let us introduce the Cartesian coordinates (x_1, x_2, x_3) in the E-cell. We locate the origin of the coordinates in the E-cell center and orient axis x_j ($j = 1,2,3$) toward the octahedron vertices (see Fig. 2). The positions of the boundary metal atoms are determined by radius vectors $\mathbf{r}_i$ ($i = 1,2,\ldots,18$). Introducing the standard notation X_j for the E-cell size along the j axis, we assume that $X_2 = X_3 = Y$ always (but $X_1 = X$ can differ from Y). The hydrogen atoms are located at symmetrical points $x_j = \pm X_j/2$ before and immediately after the E-cell formation. For symmetry reasons, we conclude that these atoms move symmetrically along the corresponding axes.

Let us consider the motion of the hydrogen atom, denoted by I on Fig. 2. Its trajectory is described by the function $x(t)$. The dynamical equation for $x(t)$ is

$$M\, d^2x/dt^2 = \sum_{j=\mathrm{II}}^{\mathrm{VI}} F_j + \sum_{i=1}^{18} G_i + f \ , \qquad (12)$$

where

F_j ($j = \mathrm{II},\ldots,\mathrm{VI}$) = hydrogen-hydrogen interaction forces acting on atom I

G_i ($i = 1,\ldots,18$) = forces of the interaction of hydrogen atom I with the boundary metal atoms

f = force of the interaction of hydrogen atom I with the remaining atoms of the crystalline lattice.

All the forces are potential, and the values of F_j and G_i are determined from Eq. (11). For example,

$$F_{\mathrm{III}} = e^2 \exp(-2\lambda x)(1 + 2\lambda x)/4x^2 \ , \qquad (13)$$

where λ is the screening parameter of the Coulomb interaction of hydrogen nuclei. Since the movements of atoms II, IV, V, and VI are symmetrical, the corresponding total force can be written as

$$F_{II} + F_{IV} + F_V + F_{VI} = 4e^2 \exp(-\lambda r)(1 + \lambda r)x/r^3 \ , \tag{14}$$

where

$$r = [x^2(t) + y^2(t)]$$

$y(t)$ = coordinate of one of the atoms II, IV, V, or VI.

The forces $G_i(x)$ can be written by analogy with Eq. (14). It is very difficult to determine the value of f by a direct summation of the forces acting on atom I from the rest of the atoms of the lattice. We are rescued from this difficulty in the following way. Let us note that before the fission of the central nucleus, atom I was at the point $x = X/2$ in an equilibrium state. We denote $f(x = X/2) = -\Phi$ and have

$$\Phi = \left[\sum_{j=II}^{VI} F_j + \sum_{i=1}^{18} G_i + G_0\right]_{x=X/2} \ , \tag{15}$$

where G_0 is the force of interaction between hydrogen atom I and the central metal atom. It is obvious that $f(x = -X/2) = \Phi$ and $f(x = 0) = 0$. We can interpolate the dependence of f on x by the function $f(x) = -2\Phi x/X$ or, in potential form,

$$f(x) = -\partial V/\partial x \quad \text{and} \quad V(x) = \Phi x^2/X \ .$$

Taking into account all of these considerations, we can write Eq. (12) as follows:

$$M\, d^2x/dt^2 = -\partial \mathrm{U}_x/\partial x \ , \tag{16}$$

where we introduce the potential of the movement along the x_1 axis:

$$\mathrm{U}_x = e^2\left[\exp(-2\lambda x)/4x + 4\exp(-\lambda r)/r + Z\sum_{i=1}^{18}\exp(-\Lambda R_i)/R_i\right] + \Phi x^2/X \ , \tag{17}$$

where

Λ = screening parameter of the Coulomb interaction of the hydrogen nucleus with metal nuclei

R_i = distance between hydrogen atom I and metal atom i.

Such considerations for x_2 and x_3 give us an analogous dynamic equation that describes the movement of one of the atoms II, IV, V, or VI in Fig. 2. Introducing the notation $y(t)$ for the coordinate of one of these atoms, we have the dynamic equation

$$M\, d^2y/dt^2 = -\partial \mathrm{U}_y/\partial y \ , \tag{18}$$

where we introduce the potential of a movement along the x_2 (or x_3) axis:

$$\mathrm{U}_y = e^2\left[\exp(-2\lambda y)/4y + 4\exp(-\lambda r)/r + \exp(-\sqrt{2}\lambda y)/\sqrt{2}y + Z\sum_{i=1}^{18}\exp(-\Lambda \tilde{R}_i)/\tilde{R}_i\right] + \Gamma y^2/Y \ . \tag{19}$$

The value of factor Γ is determined similarly to the determination of factor Φ from the condition of the equilibrium of atoms before the fission of the central nucleus.

Comparing the dynamic equation, Eq. (16), and the potential, Eq. (17), with Eqs. (18) and (19), we can interpret all these equations as the dynamic problem for one pseudoparticle that moves in two-dimensional (x, y) space. This pseudoparticle has nonisotropic mass (M for a movement along the x axis and $2M$ for a movement along the y axis) and moves in the potential field $\mathrm{U}(x, y)$ of the form

$$\mathrm{U}(x,y) = e^2\left\{\exp(-2\lambda x)/4x + 4\exp(-\lambda r)/r + \exp(-2\lambda y)/2y + \sqrt{2}\exp(-\sqrt{2}\lambda y)/y + Z\sum_{i=1}^{18}[\exp(-\lambda R_i)/R_i + 2\exp(-\Lambda \tilde{R}_i)/\tilde{R}_i]\right\} + 2\Gamma y^2/Y + \Phi x^2/X \ , \tag{20}$$

where

$$R_i = |\boldsymbol{x} - \boldsymbol{r}_i| \quad \text{and} \quad \tilde{R}_i = |\boldsymbol{y} - \boldsymbol{r}_i| \ .$$

The importance of such an interpretation of the dynamic equations, Eqs. (16) and (18), is the possibility of determining the classical distance R_0 of the closest approach of the hydrogen nuclei. The area that is accessible for the motion of the pseudoparticle is bounded by the equipotential line that passes through the initial point $(x = X/2, y = Y/2)$. The minimal distance R_0 of the points of this equipotential line from the y axis is unknown.

IV.D. Reduction of X

The movement of the pseudoparticle reduces to one dimension if it is clear *a priori* that $x(t) = y(t)$ is true. This is the case in the LiH E-cell if the pressure in the crystal is near zero. In this case, $X = Y = 8.5$ (in Hartree units), and potential U depends on x (or y) only. This function is shown in Fig. 5 (curve 1). It is assumed that $s = \lambda a = 1.9$ and $S = \Lambda a = 2.2$ in accordance with the results listed in Table VIII

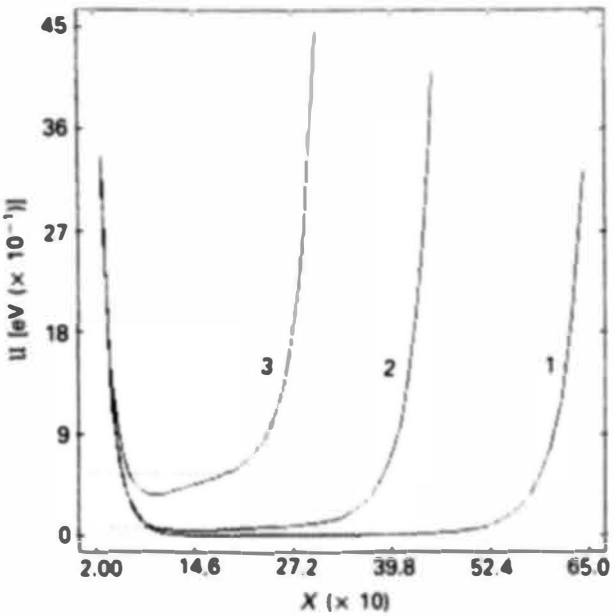

Fig. 5. E-cell potential well for one-dimensional movement of the pseudoparticle. Curves 1, 2, and 3 correspond to E-cells under pressures of 1, 30, and 300 Mbar, respectively.

for $\mathfrak{N} = 0.03$. The horizontal dotted line in Fig. 5 corresponds to the initial energy level. As can be seen, the minimal possible distance between hydrogen nuclei is characterized by $X_m = 1.8$, which is of no interest in the current context.

We can reduce X_m by the isotropic compression of a crystal. Curves 2 and 3 in Fig. 5 represent the dependence of $\mathfrak{U}$ on x for $P = 30$ and 300 Mbar, respectively. We see that the decrease in X_m is small. Even if $X_c = 3.5$ ($P = 300$ Mbar), we have $X_m = 0.7$; this is also of no interest. To obtain the desired values $X_m < 0.1$, one must achieve a compression of >1000 times, which is practically impossible.

It is more interesting to consider the nonisotropic compression of a crystalline lattice. Let us consider the compression of the crystal along one of the axes by a pressure $P =$ 30 Mbar. We assume that the volume of the E-cell reduces in the same way as in the case of an isotropic compression: i.e., to $X_1X_2X_3 = 140$. The sizes X_2 and X_3 are the same as in an uncompressed crystal ($X_2 = X_3 = 8.5$); hence, $X_1 = 2$. In this case, the motion of the pseudoparticle is two-dimensional, and the potential energy $\mathfrak{U}$ becomes a function of two variables: $\mathfrak{U} = \mathfrak{U}(x, y)$. This function is shown in Fig. 6. The initially single potential well of the E-cell is divided into two parts that are separated by the potential barrier. The origin of the latter is connected with the influence of boundary atoms, denoted by 4 and 16 in Fig. 2. These atoms push out hydrogen atom II from the segment of the y axis near the point $y = Y/2$. The same effect is caused by atom pairs (3,15), (5,7), and (2,14). The equipotential lines are depicted in Fig. 7. The most interesting region is near the boundary where $x = 0$.

In the case of nonisotropic compression, the accessible (along the x axis) region is bounded by $\min\{X\} = 0.11$, which is of much more interest than the case of isotropic compression. We can reduce the value of $\min\{X\}$ by using the hypothetical HeH crystal (with a cubic crystalline lattice) for the formation of the E-cell; there is a possibility of greater compression of the HeH by the same amount of pressure.

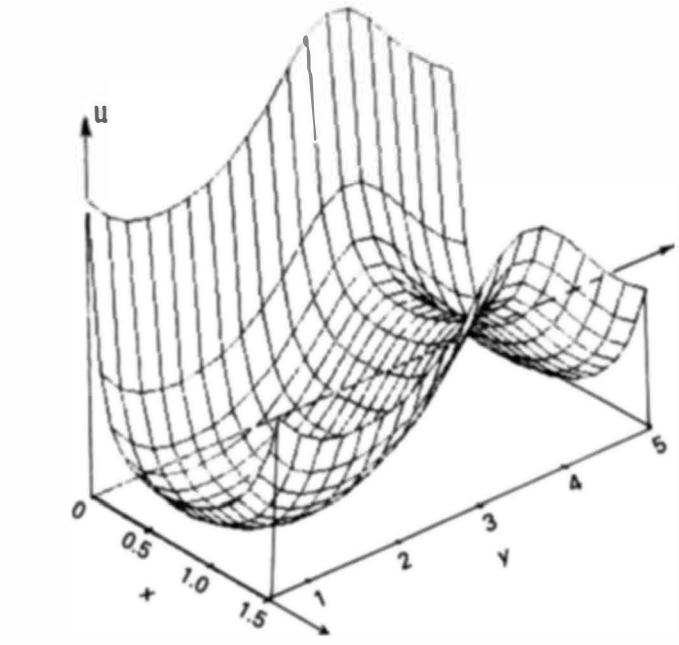

Fig. 6. E-cell potential well for two-dimensional movement of the pseudoparticle. The potential barrier divides the well into two parts. In the most favorable case, the pseudoparticle begins its movement from this barrier.

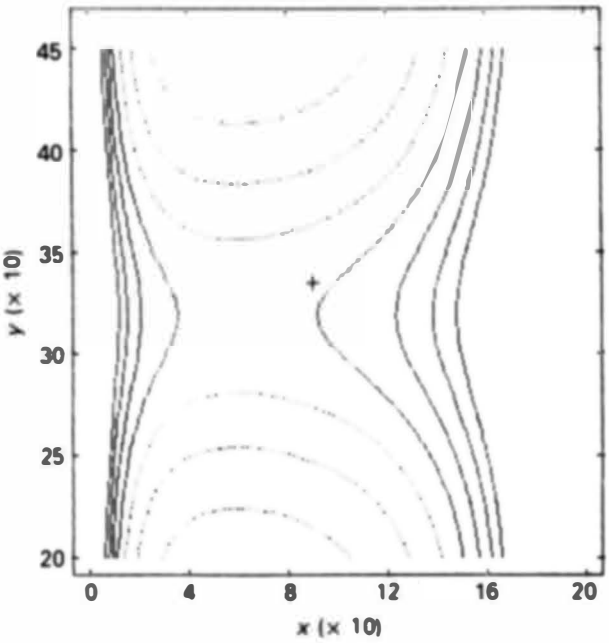

Fig. 7. Equipotential lines of the effective potential well of the E-cell for two dimensional movement of the pseudoparticle. The initial position of the pseudoparticle is marked by the plus sign.

We see a strong reduction of the distance of the closest approach of the hydrogen nuclei in the case of isotropic compression of a crystalline lattice. The physical reason for this is easy to understand. In the case of nonisotropic compression of a crystal, there is essential growth of the initial potential energy of interatomic interactions. The motion of the hydrogen nuclei in the E-cell is a collective phenomenon. The initial potential energy of six hydrogen nuclei can transform into the kinetic energy of two hydrogen nuclei in some phases of a collective motion. The possibility of approaching to distance $X_m = 0.11$ corresponds to a kinetic energy $E_m = 9$ (all in Hartree units). In usual units, $R_m \simeq 0.06$ Å and $E_m \simeq 250$ eV.

IV.E. Estimation for *W*

The estimations of the distance R_m of the closest approach of the hydrogen nuclei and the corresponding energy E_m allow us to calculate the value of W, which determines the tunneling probability (see Sec. I). We assume that the value of λ is 1.9, and we obtain the following estimations for W in LiH crystal:

1. uncompressed crystal: $W \simeq 230$
2. crystal isotropically compressed by a pressure of 30 Mbar: $W \simeq 120$
3. crystal nonisotropically compressed by a pressure of 30 Mbar: $W \simeq 44$.

In a hypothetical cubic HeH crystal, nonisotropically compressed by a pressure of 30 Mbar, $W \simeq 30$.

IV.F. Main Results

The results of the foregoing consideration allow us to draw the following conclusions:

1. It is possible to use the approximation of pairwise interaction of two atoms in the free-electron gas to investigate interactions in a polyatomic system. The electron density must be chosen so that the pressure in the gas coincides with the pressure in the initial system.

2. Within the framework of the T-F model, the parameter of the screening of the Coulomb interaction of hydrogen nuclei with atoms has the value $S = 1.9$ to 2.4 (in Hartree units). It varies weakly with pressure variations in the system.

3. By itself, a pressure increase in a crystal exerts a weak influence on the tunneling probability of hydrogen nuclei. In the case of nonisotropic compression, the energy of hydrogen nuclear collisions can be $\simeq$0.25 keV if the pressure in the crystal is in the megabar range.

4. The effect of nonisotropic compression of a crystal can make detectable the nuclear fusion reaction in a compressed crystalline hydride.

V. THE QUANTUM-MECHANICAL SCREENING OF THE COULOMB POTENTIAL IN THE E-CELL

The T-F model is suitable for a description of atoms with a large ordering number Z. The use of this model for an investigation of the hydrogen atom can furnish improper results. These results can be wrong in principle if we consider the hydrogen atom in the E-cell. If the screening of the Coulomb potential of a proton is effective enough, the width of the potential well becomes insufficient for the existence of an electron coupled state. In this case, there is an interaction of free electrons with a proton that is not described within the T-F model. It is advisable to use a strict quantum-mechanical approach for the description of electrons near hydrogen nuclei.

The main difficulties of solving the problem of quantum screening by low-energy electrons are connected with self-consistent quantum-mechanical calculations of the electron density and of the form of the potential near the positive charge in the electron background. In addition, it is still important to investigate the screening effects in the case when free electrons are characterized by a continuous distribution in the energy. In this case, we need to determine the screening as an integral (over all spectral intervals) effect.

The mathematical formulation of this problem is given in Appendix B (see also Ref. 28). We use the long-wave approximation; i.e., we assume that the electron wavelength is large enough for comparison with the radius of interaction. This approximation is more justified when the screening is more effective. Practically, this approximation reduces to neglecting all partial amplitude perturbations with nonzero angular momenta. We can assume that the results obtained with this approximation provide a lower estimation of the screening parameter.

In this section, we consider the problem of quantum-mechanical screening of the Coulomb potential as applied to the E-cell phenomena.

V.A. Screening in the E-Cell

The main equation of the theory of the quantum-mechanical screening (in view of the finiteness of the average energy of electrons) has the form:

$$d^2\mathrm{U}/dx^2 = 8\pi\eta \exp(-\kappa x)\,[\mathrm{W}_s + (\mathrm{W}_s - \mathrm{W}_c)/\kappa x]/\kappa \quad \text{(in Hartree units)}\,, \tag{21}$$

where

U = modified electrical potential [$\mathrm{U} \equiv r\cdot\varphi(r)/e$]

η = density of electron background ($\eta \equiv n_0/N_0$)

κ = value of the average wave number of the electrons

$\mathrm{W}_s, \mathrm{W}_c$ = functions that determine the perturbations of the electron density.

The real perturbation of the electron density δn is determined via W_s and W_c by

$$\delta n = n_0\cdot\eta\cdot\mathfrak{N}(x)\,,$$

where

$$\mathfrak{N}(x) = 2\cdot\exp(-\kappa x)\cdot[\mathrm{W}_s + (\mathrm{W}_s - \mathrm{W}_c)/\kappa x]/\kappa\,. \tag{22}$$

The functions W_s and W_c are determined by

$$d^2\mathrm{W}_s/dx^2 - (\kappa^2 - 2\mathrm{U}/x)\mathrm{W}_s + 2\mathrm{U}sh(\kappa x)/x = 0 \tag{23a}$$

and

$$d^2\mathrm{W}_c/dx^2 - (\kappa^2 - 2\mathrm{U}/x)\mathrm{W}_c + 2\mathrm{U}\kappa ch(\kappa x) = 2\kappa^2\mathrm{W}_s\,. \tag{23b}$$

Let us consider the screening effects in the E-cell within the shell model framework. We assume that there is one hydrogen nucleus at the center of the E-cell. The other five hydrogen nuclei are displaced on the inner shell with radius $X_s = X_c/2$. The surplus electrons leave the E-cell. This situation is described by the following set of parameters: $Z_0 = 1$, $Z_s = 5$, $Z_c = 4Z$, and $dZ = 0$. The boundary conditions for the modified electrical potential are

$$\mathrm{U}(x = 0) = 1\,,$$
$$(\mathrm{U})_{x=X_s} = 0\,,$$
$$(d\mathrm{U}/dx)_{x=X_s} = Z_s/X_s\,,$$
$$\mathrm{U}(x = X_c) = 0\,,$$

and

$$(d\mathrm{U}/dx)_{x=X_c} = Z_c/X_c\,. \tag{24}$$

The average density η of the electron gas is determined by the condition of the neutrality of the E-cell as a whole: $\eta = 3(Z_c + 1)/4\pi X_c^3$. For a perturbation of the electron density, this condition has the form

$$4\pi\eta\int_0^{X_c} dx\,x^2\mathfrak{N}(x) = 1 + Z_c\,. \tag{25}$$

This equation together with the obvious equation $\mathrm{W}_s(x=0) = \mathrm{W}_c(x=0) = 0$ are additional conditions that determine the solution of Eq. (23). It is convenient to convert the differential equation, Eq. (21), and the boundary conditions, Eq. (24), into an integral equation:

$$\mathrm{U}(x) = \mathrm{U}_n(x) - 4\pi\eta\left[x\int_x^{X_c} dx'\,x'\mathfrak{N}(x') + \int_0^x dx'\,x'^2\mathfrak{N}(x')\right]\,, \tag{26}$$

where we use the abbreviation (the potential of nuclei)

$$\mathrm{U}_n(x) = 1 + Z_c\cdot(x/X_c) + Z_s\cdot\begin{Bmatrix}(x/X_s) & \text{if } x < X_s\\ 1 & \text{if } x > X_s\end{Bmatrix}\,.$$

We solve the problem, Eqs. (21), (23), (24), and (25), of the self-consistent distribution of the electrical field and electron density by iteration. First, we choose an appropriate test function $U(x)$. In the first approximation, we solve the Eqs. (23) and (25) for $W_s(x)$ and $W_c(x)$. By inserting the first-order solution $W_s(x)$ and $W_c(x)$ into Eq. (26), we obtain the second-order solution $U(x)$, etc.

The result is shown in Fig. 8 (curves 3 and 6). We see that the electrical potential is equal to zero at a distance $X_0 \simeq 0.25$ (in Hartree units) from the central hydrogen nucleus. For comparison, two other results derived from models earlier discussed are also plotted in the same figure. We see that the quantum-mechanical effects are of importance in the E-cell phenomena investigations.

V.B. Role of the Average Energy of Electrons

The results of a more detailed analysis of the quantum-mechanical screening effects show that if the average wave number of the electrons increases, the electron density at the E-cell center increases, and thus, the screening also increases. The physical reason for this is easy to understand. If the electron's momentum increases, the uncertainty of its position decreases. Hence, the distance of the closest approach of electrons to a nucleus decreases. This effect is exactly opposite to the decrease in the Debye screening parameter with an increase in temperature.

Immediately after the transformation of a normal cell of a crystalline lattice into an E-cell, free electrons form the electronic shell of the destroyed metal atom. The average energy $\langle E \rangle$ of the free electrons in the E-cell is $\sim 16Z^{4/3}$ eV per electron (see Sec. II.B). For instance, for lithium, $\langle E \rangle \simeq 60$ eV; for boron, $\langle E \rangle \simeq 140$ eV. The average wave numbers κ that correspond to these energies are $\simeq 2$ to 3. A further increase in screening of the Coulomb potential can be connected with an increase in an average electron's energy in the E-cell. One possible path to this increase is the use of heavy elements as the hydride base. The average energy of the electrons that remain in the E-cell after the central nucleus fission is $\simeq 260$ eV for ^{17}O, for example. This corresponds to $\mathcal{E} \simeq 10$ and $\kappa \simeq 14$. In this case, calculations of the screening effects give us $X_0 \simeq 0.1$. The case of chief industrial importance is the use of elements with $Z \geq 92$. In this case, an average energy $\mathcal{E} \geq 250$ corresponds to $X_0 \simeq 0.025$.

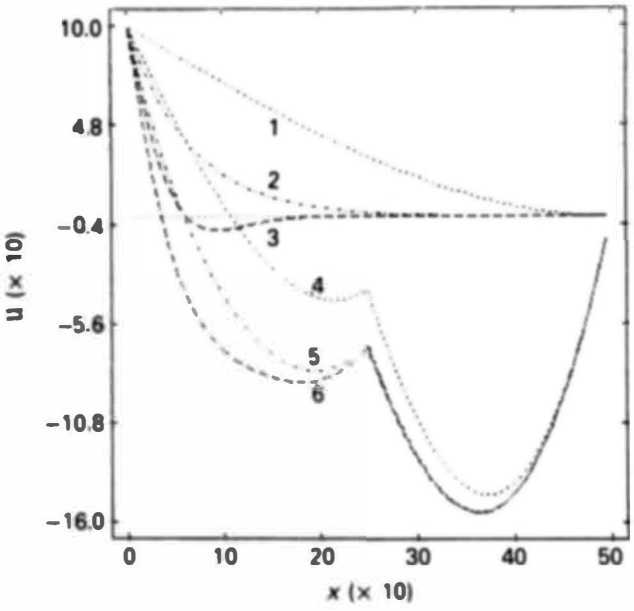

Fig. 8. Modified potential $U(x)$ distributions in the E-cell. Curves 1 and 4 correspond to a uniform electron density (curve 1 is the modified potential of the central hydrogen nucleus with one "distributed" electron, and curve 4 is the total modified potential of the electron-nuclear system of the E-cell). Curves 2 and 5 correspond to the electron density within the T-F model framework; curves 3 and 6 are determined within the LW approximation. It is assumed that $\kappa \simeq 2.5$.

It is clear that the electron temperature can be differentiated from the lattice temperature for only a short time. The question of how long a high electron temperature, which is needed for the effective screening of the Coulomb potential in the E-cell, can be maintained must be considered together with other analogous problems, such as how long the confinement of the surplus electrons exists, how long the hydrogen nuclei energy can be conserved, etc. These questions are of great importance for a separate investigation.

V.C. Qualitative Conclusions

The results of the consideration of quantum-mechanical screening effects allow us to draw the following conclusions:

1. The use of the long-wave approximation to determine wave functions of free electrons is adequate for the description of actual phenomena in the central regions of the E-cell.

2. The screening law in the E-cell differs from the Fermi law that is usually used in solid-state theory. There are differences both in the functional dependence of the potential on the distance and in the dependence of the screening parameter on the electron density.

3. The effects of quantum-mechanical screening can be important for the significant growth of the tunneling probability of hydrogen nuclei if the electron's energy is sufficiently large.

VI. THE SUMMARY EFFECT

Two main effects can significantly increase the tunneling probability of hydrogen nuclei in the E-cell. The first is the growth of the potential energy of interatomic interactions as a consequence of nonisotropic compression of a crystal. The initial potential energy of six hydrogen nuclei can be transformed into the kinetic energy of two hydrogen nuclei in some phases of the collective motion of hydrogen nuclei in the E-cell. The second effect is a significant increase in the screening of the Coulomb interaction of hydrogen nuclei in the E-cell.

These two effects act independently; hence, their influences are summed. We can use Eq. (1) to estimate the total effect. Assuming that $\mathcal{E} \simeq 9$ (see Sec. IV) and $X_0 \simeq 0.25$ (see Sec. V), we obtain $W \simeq 33$ for the T + D reaction.

A comparison of these estimations with the critical values of W (see Sec. I) shows that there is a real possibility of creating the conditions for the effective enhancement of the nuclear fusion rate. Thus, we can obtain a detectable yield of neutrons as a result of cold nuclear fusion in a solid.

It is clear that there are many effects besides the ones considered here. Some of these effects are unfavorable: the loss of energy and electrons from the E-cell, the reconstruction of

the crystalline lattice under high compression, the contamination of the hydride by the products of nuclear reactions, etc. However, the existence of some favorable effects is also possible: the formation of quasi-molecular structures[25] in the E-cell and Bose-condensation phenomenon in a nonuniform field.[27]

VII. CONCLUDING REMARKS

The conclusions resulting from the consideration of separate E-cell phenomena are listed in the corresponding sections of this technical note. It is expedient to discuss the conclusions as a whole.

The main result is the exposure of the existence of a new physical object called the E-cell. In the E-cell, there are physical phenomena, each of which contributes to an increase in the nuclear fusion reaction rate. The combination of these phenomena makes it possible to obtain a detectable yield of neutrons as a result of cold nuclear fusion in a solid.

These conclusions are the result of a theoretical consideration of the possible phenomena in the E-cell, and for this reason, they have a rather speculative character. We may develop more exact models and improve the corresponding methods. However, the results would not be more reliable than those described herein. The only way to confirm or to disprove our conclusions is to execute special-purpose experiments. We may say that the potentialities of the theory are exhausted now. The theoretical approach has given us the leading considerations. The rest is a matter of experimental physics.

APPENDIX A

THE T-F MODEL IN THE E-CELL INVESTIGATION

The basic equations of the T-F statistical model are as follows[26,35-37]:

1. The electron density n at a point $\boldsymbol{r}$ is related to the maximum possible momentum p at that point by

$$3\pi^2 n = (p/\hbar)^3 \ . \tag{A.1}$$

2. The maximum possible momentum p depends on the electrical potential φ as follows:

$$p^2/2m - pe^2/\hbar^2 - e\varphi = const \ , \tag{A.2}$$

where the second term on the left side of the equation takes the exchange effects into account.

3. The electrostatic Poisson equation for the potential U has the following form:

$$\Delta\varphi = 4\pi\left[en - \sum_i e_i\delta(\boldsymbol{r} - \boldsymbol{r}_i)\right] \ . \tag{A.3}$$

Using the freedom of choice of the potential zero level, we can exploit the "shift" potential $\tilde{\varphi}$ and set the constant on the right side of Eq. (A.2) to $-me^4/2\pi^2\hbar^2$. We solve the resulting equation as follows:

$$p = me^2/\pi\hbar + (2me\tilde{\varphi})^{1/2} \ . \tag{A.4}$$

Substituting Eq. (A.4) for Eq. (A.1) and using the resulting expression for Eq. (A.3), we obtain the equation for $\tilde{\varphi}(r)$ only:

$$\Delta\tilde{\varphi} = \frac{4\pi}{3\pi\hbar^3}\cdot\left[\frac{me}{\pi\hbar} + (2me\tilde{\varphi})^{1/2}\right]^3 - 4\pi\cdot\sum_i e_i\delta(\boldsymbol{r} - \boldsymbol{r}_i) \ . \tag{A.5}$$

This equation is used to consider the parameters of the compressed neutral atoms and the charged negative ions (Sec. II). This equation is also used to investigate, within the shell model framework, the E-cell structure (Sec. III). These cases differ by the boundary conditions at the E-cell central point ($r = 0$) and on the boundary surface. In the first case (consideration of atoms and ions), we have $\tilde{\varphi}(r \to 0) \to eZ/r$.

The variations of the potential φ near the outer boundary of atoms correspond to the escape from the neutral system:

$$(d\tilde{\varphi}/dr)_{r=R} = (d\varphi/dr)_{r=R} = 0 \ .$$

Near the outer boundary of negative ions, we have

$$(d\tilde{\varphi}/dr)_{r=R} = (d\varphi/dr)_{r=R} = e/R^2 \ .$$

We do not know the value of the shift potential $\tilde{\varphi}$ on the outer boundary of our system. This value is determined in the process of solving the corresponding problem. We can determine the connection between φ and $\tilde{\varphi}$ by

$$\varphi(r) = \begin{cases} \tilde{\varphi}(r) - \tilde{\varphi}(r = R_a) & \text{in the case of neutral atoms} \\ \tilde{\varphi}(r) - \tilde{\varphi}(r = R_i) - e/R_i & \\ & \text{in the case of negative ions} \ . \end{cases}$$

In the investigation of the E-cell as a whole, the different boundary conditions correspond to the different stages of E-cell evolution. For example, there can be a different number Z_0 of electrical charges at the E-cell center: Before the E-cell formation, $Z_0 = Z$; immediately after, $Z_0 = 0$. Some of the hydrogen nuclei that belong to the E-cell system can get to the central volume of the E-cell in the course of E-cell evolution. Outside this volume, we can determine a potential $\tilde{\varphi}$, using Eq. (A.6) with the changing $Z \to Z_0$, where the value of Z_0 can vary from 0 to 6.

The outer boundary of the E-cell, within the shell model framework, is a uniformly charged sphere (total charge is $Z_0 = 4Z$), and it determines the jump of a derivative $d\varphi/dr$ on the boundary:

$$(d\varphi/dr)_{r=R_c} \equiv (d\varphi/dr)_{r=R_c+0} - (d\varphi/dr)_{r=R_c-0} = -4eZ/R_c^2 \ .$$

Before the fission of the central nucleus, the cell is neutral; hence,

$$(d\varphi/dr)_{r=R_c+0} = 0$$

and

$$(d\varphi/dr)_{r=R_c-0} = 4eZ/R_c^2 \ .$$

If surplus electrons are confined in the E-cell, the total E-cell charge is Z, and we have

$$(d\varphi/dr)_{r=R_c+0} = eZ/R_c^2$$

and

$$(d\varphi/dr)_{r=R_c-0} = 5eZ/R_c^2 \ .$$

The derivative $(d\varphi/dr)_{r=R_c-0}$ returns to the initial value in Eq. (A.7) during these stages of E-cell evolution, when surplus electrons leave the E-cell.

The boundary value of the shift potential $\tilde{\varphi}(r = R_c)$ is determined in the process of solving the corresponding problem. We can determine the connection between φ and $\tilde{\varphi}$ by

$$\varphi(r) = \begin{cases} \tilde{\varphi}(r) - \tilde{\varphi}(r = R_c) - eZ/R_c \\ \quad \text{if surplus electrons are confined in the E-cell} \\ \tilde{\varphi}(r) - \tilde{\varphi}(r = R_c) \\ \quad \text{if surplus electrons leave the E-cell} \; . \end{cases}$$

When we investigate the E-cell inner structure within the shell model framework (see Sec. III), we assume that the hydrogen nuclear charge is distributed uniformly on a spherical surface (called the hydrogen shell) of radius R_s ($R_s < R_c$). The summary charge Z_s of these nuclei is equal to $6e$ before and immediately after the E-cell formation. During E-cell evolution, some of these nuclei may move to the E-cell center. If the number of displaced nuclei is Z_0, then the charge of the hydrogen shell is $e(6 - Z_0)$. It is convenient to solve the differential Eq. (A.5) within two regions: $0 < r < R_s$ and $R_s < r < R_c$. On the boundary $r = R_s$, the conditions for potential are

$$[\varphi]_{r=R_s} = 0 \quad \text{and} \quad [d\varphi/dr]_{r=R_s} = -eZ_s/R_s^2 \; .$$

Let us consider the energy characteristics of atoms, ions, and the E-cell as a whole. The importance of this consideration is determined by the following circumstance. By calculating the energy of different configurations of a considered system, we can predict the direction of the evolution of this system. This evolution is direct to the configuration with the minimum total energy E_{tot}. The value of E_{tot} is the sum of four components[35]:

1. *The kinetic energy of electrons*: In the degenerated electron gas, an average kinetic energy $\langle E \rangle$ is related to the maximum momentum p of electrons by $\langle E \rangle = 3p^2/10m$. Hence, the kinetic energy of the electron system is determined by the integral

$$E_{kin} = (3/10m) \cdot \int np^2 \, dv$$

$$= \int p^5 \, dv/(10m\pi^2\hbar^3)$$

$$= \int \left[\frac{me}{\pi\hbar} + (2me\tilde{\varphi})^{1/2} \right]^5 dv/(10m\pi^2\hbar^3) \; .$$

2. *The potential energy of electrons*: According to the common rules (see, e.g., Ref. 35), the total potential φ of an electrical field should be divided in two parts ($\varphi = \varphi_e + \varphi_n$) to calculate the potential energy of electrons. The part φ_e is the potential of the electrons, and φ_n is the potential of the nuclei.

If we consider atoms or ions, then $\varphi_n(r) = eZ/r$. If we consider the *E*-cell, we must take into account the potential of the central nuclei $\varphi_{n0} = eZ_0/r$, the potential of the charged boundary $\varphi_{hb} = 4eZ/R_c$ (within the shell model framework), and the potential of the inner hydrogen shell:

$$\varphi_{ns} = \begin{cases} eZ_s/R_s & \text{if } r < R_s \\ eZ_s/r & \text{if } r > R_s \; . \end{cases}$$

Thus, the electrical potential of nuclei in the E-cell is the sum

$$\varphi_n = \varphi_{n0} + \varphi_{nc} + \varphi_{ns} \; .$$

The potential energy of electrons is determined by the integral

$$E_{e\,pot} = -(e/2) \cdot \int n\varphi_e \, dv - e \cdot \int n\varphi_n \, dv$$

$$= -(e/2) \cdot \int n(\varphi + \varphi_n) \, dv \; . \qquad \text{(A.6)}$$

Let us emphasize that we must use the true (not shift) potential φ in these calculations.

3. *The change-exchange energy*: The addition to the energy of the E-cell electron subsystem, accounting for the change-exchange effects, is determined (see, e.g., Ref. 23) by the integral

$$E_{ex} = (3e^2/4\pi\hbar) \cdot \int np \, dv$$

$$= (e^2/4\pi^3\hbar^4) \cdot \int p^4 \, dv$$

$$= (e^2/4\pi^3\hbar^4) \cdot \int \left[\frac{me}{\pi\hbar} + (2me\tilde{\varphi})^{1/2} \right]^4 dv \; .$$

4. *The potential energy of the Coulomb interaction of nuclei*: We take into account the potential energy of the Coulomb interaction of nuclei with electrons in Eq. (A.6). Hence, the addition to the potential energy of the E-cell electron-nuclear system is the energy of the Coulomb interaction of nuclei:

$$E_{n\,pot} = e^2(Z_0Z_s/R_s + Z_0Z_c/R_c + Z_sZ_c/R_c) \; .$$

The total energy of the electron-nuclear system is thus

$$E_{tot} = E_{kin} + E_{ex} + E_{e\,pot} + E_{n\,pot} \; .$$

This value can vary during E-cell evolution. The differences δE_t of the values of E_{tot} that characterize different stages of E-cell evolution can contribute to the kinetic energy of hydrogen nuclei. Hence, we may consider the value of δE_t as an estimation of the hydrogen nuclei collision energy. During the late stages of E-cell evolution, the hydrogen nuclear kinetic energy transfers from the E-cell electron-nuclear system to the crystalline lattice.

The determination of the energy components of the electron-nuclear system allows us to determine the pressure P necessary to compress the considered system to the set size.

We can use the theorem of virial (see Ref. 35) if we consider squeezed atoms or ions. In these cases, we have

$$P = (2E_{kin} + E_{ex} + E_{e\,pot})/3V_{a,i} \; . \qquad \text{(A.7)}$$

If we consider the E-cell as a whole, we must take into account the existence of nuclei in the volume and on the border of the E-cell. Within the shell model framework, the variations of the nuclear potential energy comply with the conditions of the theorem of virial; hence, we have an analog of Eq. (A.7):

$$P = (2E_{kin} + E_{ex} + E_{e\,pot} + E_{n\,pot})/3V_c \; , \qquad \text{(A.8)}$$

where V_c is the volume of the E-cell. Within the shell model framework,

$$V_c = 4\pi R_c^3/3 \; .$$

In Sec. IV, we investigate the E-cell phenomena within the discrete model framework. We exploit the energy characteristics of atoms in a free-electron gas of density n_0. Atoms

are compressed by the pressure that is created in the gas. The pressure P is related to electron density n_0 by

$$P = (3\pi^2)^{2/3}\hbar^2 n_0^{5/3}/5m - (3/\pi)^{1/3}e^2 n_0^{4/3}/4 \ . \quad (A.9)$$

The first term on the right side of the equation is the usual term[38] for degenerated electron gas; the second term is an addition that takes the exchange effects into account.[39]

The potential variations at point r are determined by the amount by which the electron density exceeds its background value:

$$\Delta\varphi = 4\pi e(n - n_0) \ .$$

The determination in Eq. (A.1) of the electron density n via the maximal momentum p is true in the considered case, but the relation between p and φ is determined by

$$(p - p_1)^2 - (p_0 - p_1)^2 = 2me\varphi \ .$$

According to this equation, if $\varphi \to 0$, $p \to p_0$, where p_0 is related to n_0 by Eq. (A.1) and $p_1 = me^2/\pi\hbar$.

In the case of an atom in electron gas, the relation between the shift potential $\tilde{\varphi}$ and the true potential φ is clear *a priori*:

$$\tilde{\varphi} - \varphi = (p_0 - p_1)^2/2me \ .$$

The equation for $\tilde{\varphi}(r)$ has the form

$$\Delta\tilde{\varphi} = \frac{4\pi}{3\pi\hbar^3} \cdot \{[p_1 + (2me\tilde{\varphi})^{1/2}]^3 - p_0^3\} \ . \quad (A.10)$$

Boundary conditions for $\tilde{\varphi}$ have the form

$$\tilde{\varphi}(r \to 0) \to eZ/r \ ,$$

$$\tilde{\varphi}(r = R_a) = (p_0 - p_1)^2/2me \ ,$$

and

$$(d\tilde{\varphi}/dr)_{r=R_a} = 0 \ . \quad (A.11)$$

The solution of the boundary problem in Eqs. (A.10) and (A.11) determines the structure of an atom in the free-electron gas.

As in the investigations of the E-cell evolution, the analysis of the variation in atomic energy in the considered case gives us important information about the E-cell phenomena (see Sec. IV).

The total energy of the electron system of an atom in free-electron gas is determined by the integral

$$E_{e\,tot} = \int \{(3/10m)(np^2 - n_0p_0^2) - (3e^2/4\pi\hbar)(np - n_0p_0) - (e/2)[(n + n_0)\varphi + (n - n_0)\varphi_n]\}\, dv \ . \quad (A.12)$$

The first two terms in the braces are the kinetic and exchange energies of electrons with the deduction of the corresponding components of the energy of the electron gas. The last term is the potential energy of the electrons. The function $\varphi_n = Ze/r$ is the Coulomb potential of a nucleus. The given form of the term of a potential energy requires an explanation.

It is assumed that the potential energy of electrons is the sum of the potential energy of additional (to background) electrons E_{pot1} and the potential energy of the background electrons E_{pot2}. The density of the additional electrons is $n - n_0$, and their potential energy is

$$E_{pot1} = -e \cdot \int (n - n_0)(\varphi_n + \varphi_e/2)\, dv \ .$$

A factor of $\frac{1}{2}$ in the second term of the integrand is needed to eliminate repeated accounting of the energy of electron-electron interactions (see Ref. 35). This factor is unnecessary if we calculate the potential energy of the background electrons (they do not create an electrical field); therefore,

$$E_{pot2} = -e \cdot \int n_0\varphi\, dv \ .$$

The sum $E_{pot1} + E_{pot2}$ gives us the total potential energy of the electrons in the form of the last term of Eq. (A.12).

In numerical calculations, we use the Hartree system of units (see Sec. II.A). Let us write the main equations of the T-F model in this system.

The modified potential U is determined by $\mathrm{U} = \varphi r/e$, and modified shift potential $\tilde{\mathrm{U}}$ is determined by $\tilde{\mathrm{U}} = \tilde{\varphi} r/e$. The equation for $\tilde{\mathrm{U}}$ has the form

$$d^2\mathrm{U}/dx^2 = \alpha x[\beta + (\mathrm{U}/x)^{1/2}]^3 \ , \quad (A.13)$$

where

$$\alpha \equiv 2^{7/2}/3\pi \simeq 1.20 \quad \text{and} \quad \beta \equiv 1/2^{1/2}\pi \simeq 0.225 \ .$$

The total energy of the electron system of an atom or ion is determined by the integral

$$\mathcal{E}_t = \int_0^{X_a} \{\alpha_k[\beta + (\mathrm{U}/x)^{1/2}]^5 - \alpha_e[\beta + (\mathrm{U}/x)^{1/2}]^4 - \alpha_p[\beta + (\mathrm{U}/x)^{1/2}]^3 \cdot [\mathrm{U}/x + \Phi(x)]\} x^2\, dx \ , \quad (A.14)$$

where $\Phi = Z/x$ is the potential of nucleus, and the constants are

$$\alpha_k = 2^{7/2}/5\pi \ ,$$

$$\alpha_e = (2/\pi)^2 \ ,$$

and

$$\alpha_p = 2^{5/2}/3\pi \ .$$

The pressure $\mathfrak{P}$ is determined by the components of energy by

$$\mathfrak{P}(X) = (2\mathcal{E}_k + \mathcal{E}_e + \mathcal{E}_p)/X^3 \ .$$

The inverse function $X(\mathfrak{P})$ determines the size of an atom, an ion, or the E-cell as a whole as a function of the pressure $\mathfrak{P}$ in a crystal.

The two-point boundary problem to determine the modified potential is solved by choosing the initial (for $x = 0$) derivation of the function $\mathrm{U}(x)$. This method is known as the reduction of a two-point boundary value problem to an initial-value problem (see, e.g., Ref. 40).

Examples of the results of calculations of the structure of a compressed atom and ion ($Z = 3$) are shown in Fig. A.1. The dimensionless radius (atom or ion) is equal to 1.5. The dashed lines represent the distribution of the modified shift potential $\tilde{\mathrm{U}}(x)$ for an atom (curve 1) and an ion (curve 2), and the dotted lines represent the distribution of a true modified potential $\mathrm{U}(x)$ for an atom (curve 3) and an ion (curve 4).

The corresponding distributions of the modified dimensionless electron density $\nu(x) \equiv 4\pi x^2\mathfrak{N}(x)$ are shown in Fig. A.1 by solid lines for an atom (curve 5) and an ion (curve 6). In the case considered ($X = 1.5$), the total energy is equal to -304 eV for an atom and -271 eV for an ion. So, the transformation of a neutral atom into a negative ion requires an energy expenditure of $\simeq$33 eV. A pressure of $\sim$11 Mbar is required to compress an atom to a size $X = 1.5$ ($R_a = 0.79$ Å).

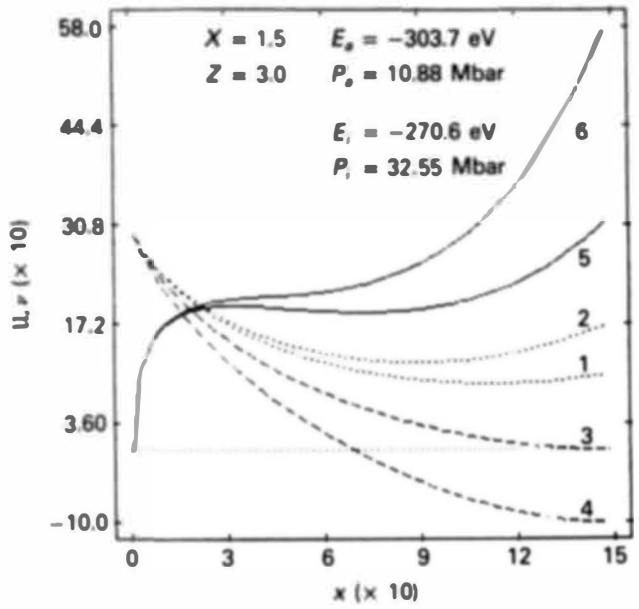

Fig. A.1. Potential U (curves 1 through 4) and density ν (curves 5 and 6) distributions for a lithium neutral atom (curves 1, 3, and 5) and negative ion (curves 2, 4, and 6). Both are compressed to radius $X = 1.5$ ($R = 0.79$ Å). The necessary pressure is ≃11 Mbar for an atom and ≃30 Mbar for an ion. The total energy is approximately −304 eV for an atom and approximately −271 eV for an ion.

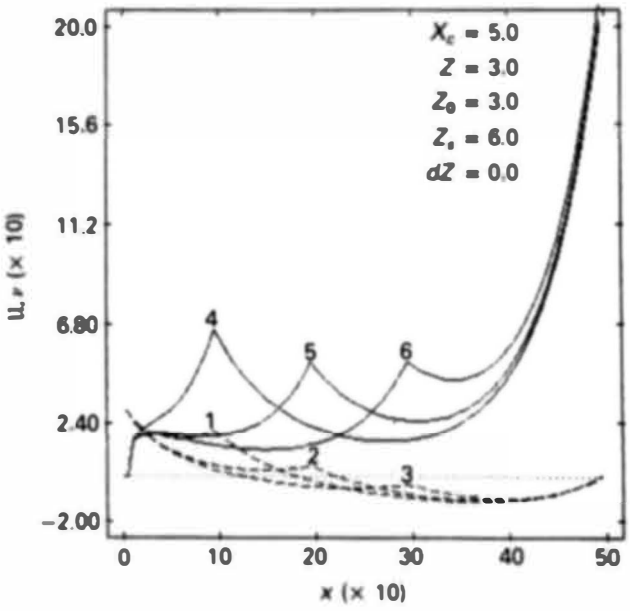

Fig. A.2. E-cell structure. The various pairs of curves (1 and 4, 2 and 5, and 3 and 6) correspond to various values of the radius (X_s = 1, 2, and 3, respectively) of the inner hydrogen shell. The solid lines show the modified electron density, and the dashed lines show the modified potential distributions. The E-cell radius is $X_c = 5$ (R_c = 2.65 Å).

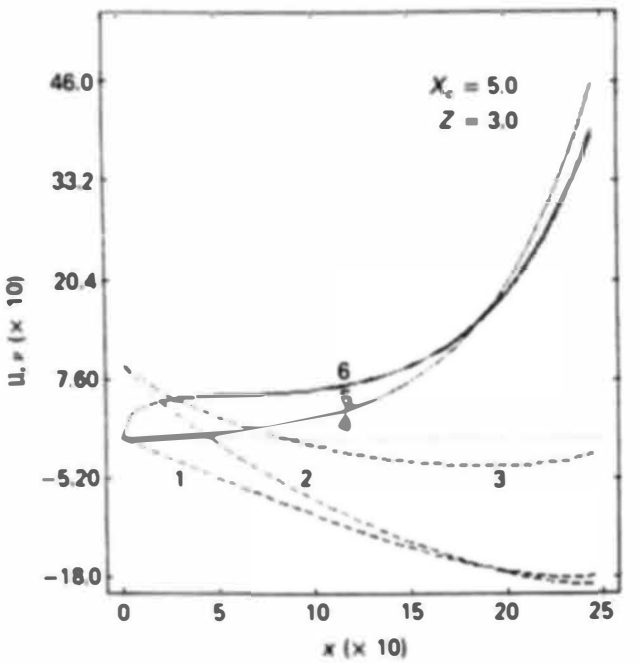

Fig. A.3. Structure of the E-cell inner area ($0 \le x \le X_s$) during various stages of E-cell evolution. The solid and dashed lines show the electron density and potential distributions, respectively. The E-cell parameters are as follows (see Table III): $Z_0 = 0$, $Z_s = 6$, and $dZ = 3$ (curves 1 and 4); $Z_0 = 1$, $Z_s = 5$, and $dZ = 3$ (curves 2 and 4); and $Z_0 = 1$, $Z_s = 5$, and $dZ = 0$ (curves 3 and 6).

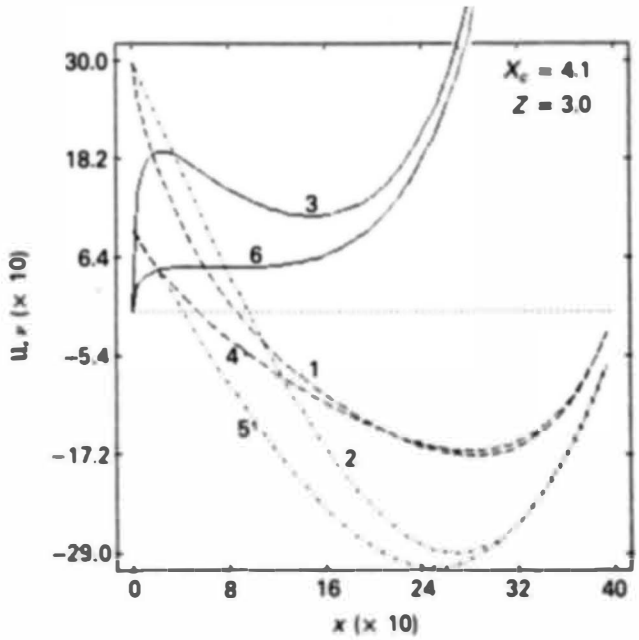

Fig. A.4. A comparison of the results of the E-cell structure analyses in two approximation frameworks. The dash-dotted lines show the potential distribution in the E-cell with a uniform electron density (see Sec. II.C) (curve 1 corresponds to $Z_0 = 3$, and curve 4 corresponds to $Z_0 = 1$). The dashed lines show the potential distribution in the E-cell with the electron density (solid lines) determined within the T-F model framework (curves 2 and 3 correspond to $Z_0 = 3$, and curves 5 and 6 correspond to $Z_0 = 1$).

The results of the investigation of the E-cell structure are shown in Fig. A.2. The dashed lines represent the distribution of the modified potential $U(x)$ for a normal cell of size $X_c = 5$ in a LiH crystal ($Z = 3$). The corresponding distributions of the modified dimensionless electron density $\nu(x)$ are shown by solid lines. The E-cell structure (the modified potential distribution) is shown in Fig. A.3. Curves 1, 2, and 3 correspond to the E-cell immediately after its formation ($Z_0 = 0$, $dZ = Z$), after the displacement of a hydrogen nucleus into the E-cell center ($Z_0 = 1$, $dZ = Z$), and after the loss of surplus electrons from the E-cell ($Z_0 = 1$, $dZ = 0$).

For future reference, we show data on the distribution of the potential and electron density in the E-cell matched with an inner H-shell with a boundary surface. These results are shown in Fig. A.4.

APPENDIX B

QUANTUM-MECHANICAL SCREENING

We *a priori* confess that the quasi-classical approximation is inapplicable to the problem of the Coulomb potential screening. Indeed, a quasi-classical wave function has an amplitude factor $p^{-1/2}$ (where p is the momentum of the particles), which describes the decrease in the free-electron density near a nucleus. It is easy to see that a strict solution of the quantum-mechanical problem leads us to the exactly opposite conclusion: There is an increase in the free-electron density above the potential well.

Let us consider the model problem of slow particle interaction with a spherical potential well of depth U_0 and radius R in the limiting case where the velocities of the particles are so small that their wavelength is large compared with radius R (i.e., for wave vector k, $kR \ll 1$), and their energy is small compared with the field U_0 within that radius. It is known (see, e.g., Ref. 17) that in this case, the perturbations of all partial amplitudes with nonzero orbital angular moments $\mathcal{L}$ are small in comparison with the perturbation of partial amplitudes with $\mathcal{L} = 0$. We can determine the wave function ψ_k of particles outside the well by

$$\psi_k = \sin(kr + \delta)/kr \ ,$$

and inside the well by

$$\psi_k = A \sin(Kr)/kr \ ,$$

where

$$k = (2mE)^{1/2}\hbar \quad \text{and} \quad K = [2m(E - U_0)]^{1/2}/\hbar \ .$$

The boundary conditions at the point $r = R$ determine the amplitude of the wave function ψ_k inside the well:

$$A = \{[1 + tg^2(KR)]/[(K/k)^2 + tg^2(KR)]\}^{1/2} \ .$$

We see the increase in the density of particles at the point $r = 0$. This increase is characterized by the ratio

$$\alpha = (AK/k)^2 = \{1 - [1 - (k/K)^2]\sin^2(KR)\}^{-1} \ .$$

The function $\alpha(E)$ reaches a maximum ($\max\{\alpha\} = |U_0|/E$) when $KR = \pi/2$. If the interacting potential is the Coulomb potential and the interacting particles are electrons, an increase of density leads to an increase in the screening effects.

The main difficulties in solving the problem of quantum-mechanical screening by low-energy electrons are connected with self-consistent quantum-mechanical calculations of the electron density and of the form of the potential near the positive charge in the electron background. In addition, it is still important to investigate the screening effects in the case when free electrons are characterized by a continuous distribution in energy. In this case, we need to determine the screening as an integral (over all spectral intervals) effect.

We use the long-wave approximation; i.e., we assume that the electron wavelength is large enough for comparison with the radius of interaction. The better this approximation is justified, the more effective the screening is. Practically, this approximation reduces to the neglect of all partial amplitude perturbations with nonzero angular momenta. We can assume that the results obtained within this approximation framework provide a lower estimation of the screening parameter. It is clear that accounting for partial waves by nonzero angular momentum can increase screening effects.

The potential of electrical field is determined as a spherical symmetrical solution of Poisson's electrostatical equation:

$$\Delta\varphi = 4\pi e(n - n_0) \tag{B.1}$$

with the boundary conditions

$$\lim[r\varphi(r)] = e \quad \text{and} \quad \lim[r\varphi(r)] = 0 \ . \tag{B.2}$$

Let us introduce the distribution function F of electrons on values of wave vectors k and wave functions $\psi_k(r)$ of electrons with this wave vector. Using these functions, we can determine the electron density:

$$n(r) = \int_0^\infty F(k)|\psi_k(r)|^2\, dk \ .$$

We have the Schrödinger equation for the wave functions $\psi_k(r)$:

$$\Delta\psi_k + \left(k^2 + \frac{2me}{\hbar^2}\cdot\varphi\right)\psi_k = 0 \ . \tag{B.3}$$

We choose the solution of this equation for the free electrons (i.e., for the case $\varphi = 0$) in the form $\psi_k(r) = \sin(kr)/kr$. So we have

$$n_0(r) = \int_0^\infty F(k)\sin(kr)^2/(kr)^2\, dk \ .$$

Correspondingly, we normalize the wave function $\psi_k(r)$ and distribution function $F(k)$ to obtain

$$\lim_{r\to\infty}\{kr\psi_k(r)\} = \sin(kr + \delta) \tag{B.4}$$

and

$$\int_0^\infty F(k)\, dk = n_0 \ . \tag{B.5}$$

The equation for $\varphi(r)$ thus has the form

$$\Delta\varphi = 4\pi e\int_0^\infty F(k)\,[|\psi_k(r)|^2 - \sin(kr)^2/(kr)^2]\, dk \ . \tag{B.6}$$

The system of Eqs. (B.3) and (B.6) together with the boundary conditions in Eqs. (B.2) and (B.4) determine the self-consistent space distribution of the electrical potential and the electron density near the positive charge.

It is convenient to use the dimensionless Hartree units (see Sec. I):

$$x = r/a \ ,$$

$$K = ka \ ,$$

$$\phi = a\varphi/e \ ,$$
$$\mathcal{U} = x\phi \ ,$$
$$\mathcal{V}_k = x\psi_k(x) \ ,$$

and

$$\eta = n_0/N_0 \ .$$

From the system of Eqs. (B.3) and (B.6), we have for the new unknown variable functions $\mathcal{U}$ and $\mathcal{V}_k$ the equations

$$d^2\mathcal{U}/dx^2 = (4\pi\eta/x) \cdot \int_0^\infty f(K)\,[\mathcal{V}_k^2(x) - \sin(Kx)^2/(Kx)^2]\,dK \quad \text{(B.7)}$$

and

$$d^2\mathcal{V}_k/dx^2 + [K^2 + 2\mathcal{U}(x)/x]\mathcal{V}_k = 0 \ , \quad \text{(B.8)}$$

where the dimensionless function of distribution is normalized according to

$$\int_0^\infty f(K)\,dK = 1 \ . \quad \text{(B.9)}$$

The boundary conditions for $\mathcal{U}(x)$ and $\mathcal{V}_k(x)$ are

$$\mathcal{U}(x=0) = 1 \ , \quad \mathcal{U}(x\to\infty) \to 0 \ , \quad \text{(B.10)}$$

and

$$\mathcal{V}_k(x=0) = 0 \ , \quad \mathcal{V}_k(x\to\infty) \to \sin(Kx+\delta)/K \ . \quad \text{(B.11)}$$

Equation (B.8) has no analytical solution in the case of an arbitrary dependence of $\mathcal{U}$ on x. The use of the numerical solution of Eq. (B.8) leads us to the necessity to summarize a large number of oscillating functions in Eq. (B.7). This cannot be done with the required accuracy.

We can use some general results of the quantum theory of the potential scattering of particles (see Refs. 41 and 42).

It is convenient to convert the differential equation, Eq. (B.8) with the boundary condition of Eq. (B.11), into an integral equation:

$$K\cdot\mathcal{V}_k(x) = \sin(Kx) - 2\cdot\int_0^\infty dy \sin[K(x-y)] \times \mathcal{V}_k(y)\mathcal{U}(y)/y \ . \quad \text{(B.12)}$$

We search for a solution of Eq. (B.12) in the form

$$K\cdot\mathcal{V}_k(x) = \sin(Kx) + \int_0^x dy \sin(Ky) I(x,y) \ . \quad \text{(B.13)}$$

Let us now insert Eq. (B.13) into Eq. (B.12). This yields an integral equation satisfied by $I(x,y)$:

$$I(x,y) = \int_{(x-y)/2}^{(x+y)/2} dt \left[\frac{\mathcal{U}(t)}{t} + 2\cdot\int_0^{(x-y)/2} ds \times \frac{\mathcal{U}(t+s)}{(t+s)} I(t+s, t-s) \right] \ . \quad \text{(B.14)}$$

Note the remarkable fact that the kernel function $I(x,y)$ in Eq. (B.13) does not depend on wave vector K. Hence, Eq. (B.13) for the solution of $\mathcal{V}_k(x)$ can be inserted into Eq. (B.7). We then have

$$d^2\mathcal{U}/dx^2 = (4\pi\eta/x)\cdot\int_0^x dy\, I(x,y) \times \left[2G(x,y) + \int_0^x dt\, I(x,t) G(y,t) \right] \quad \text{(B.15)}$$

when we use the abbreviation

$$G(x,y) = \int_0^x dK f(K) \sin(Kx)\sin(Ky)/K^2 \ . \quad \text{(B.16)}$$

The formal solution of Eq. (B.15) with the boundary condition in Eq. (B.10) has the form

$$\mathcal{U}(x) = 1 - 8\pi\eta \left[x\int_x^\infty dx'\, R(x') + \int_0^x dx'\, x' R(x') \right] \ , \quad \text{(B.17)}$$

where

$$R(x) \equiv (1/x)\int_0^x dy\, I(x,y) \times \left[G(x,y) + \left(\frac{1}{2}\right)\int_0^x dt\, I(x,t) G(x,t) \right] \ .$$

The system of integral equations, Eqs. (B.14) and (B.17), is in principle simpler for analysis and for a solution than the initial system. For example, the latter system can be solved (numerically at any rate) by iterations. In the case of an arbitrary spectral distribution of electrons, it is the only method of analysis for this problem. In some cases, however, we can convert the integral equations, Eqs. (B.14) and (B.17), into a system of differential equations with corresponding boundary conditions. Let us consider some examples.

Note that we consider the problem within the long-wave approximation framework. The characteristic values of the wave vector of electrons K_0 and of potential hole width x_0 are small, so their product is small, too: $K_0 x_0 < 1$. If $K_0 x_0 \ll 1$, we can use the expansion $\sin(Kx) \simeq Kx$.

Let us insert this expansion into Eq. (B.16), taking into account the normalizing equation, Eq. (B.9). It then follows that

$$d^2\mathcal{U}/dx^2 = 8\pi\eta\mathcal{W}(x)\,[1 + \mathcal{W}(x)/2x] \ , \quad \text{(B.18)}$$

where

$$\mathcal{W}(x) \equiv \int_0^x dy\, y I(x,y) \ .$$

The function $\mathcal{W}(x)$ is the solution of some differential equation. We can write this equation, noting that the kernel function $I(x,y)$ satisfies the partial differential equation, as follows:

$$\frac{\partial^2 I}{\partial x^2} - \frac{\partial^2 I}{\partial y^2} + 2\,\frac{\mathcal{U}(x)}{x} I(x,y) = 0 \ . \quad \text{(B.19)}$$

Let us multiply Eq. (B.19) by y, integrate from $y = 0$ to $y = x$, and use the integration of the second term by parts. The result is the differential equation for the function $\mathcal{W}(x)$:

$$d^2\mathcal{W}/dx^2 + 2\mathcal{U}(x)\,[1 + \mathcal{W}(x)/x] = 0 \ . \quad \text{(B.20)}$$

The boundary conditions for $\mathcal{W}(x)$ are

$$\mathcal{W}(x=0) = 0 \quad \text{and} \quad \mathcal{W}(x\to\infty) \to 0 \ . \quad \text{(B.21)}$$

Equations (B.18) and (B.20) together with the boundary conditions in Eqs. (B.10) and (B.21) form the boundary problem. The solution of the latter determines the self-consistent distributions of the electrical potential and the electron density near a positive charge that is displaced in the free-electron background.

If we neglect the nonlinear terms in Eqs. (B.18) and (B.20), the solution of this boundary problem is

$$\mathfrak{U}(x) = \exp(-Sx)\cos(Sx)$$

and

$$\mathfrak{W}(x) = \exp(-Sx)\sin(Sx)/S^2 \ , \qquad \text{(B.22)}$$

where

$$S_q = (4\pi\eta)^{1/4} \ . \qquad \text{(B.23)}$$

To determine the role of the nonlinear terms in the system of Eqs. (B.18) and (B.20), we note that these equations can be considered as Euler's equations, which are determined as the minimum of the functional

$$\mathcal{L} = \int_0^\infty dx \left[\frac{1}{2} (d\mathfrak{U}/dx)^2 - 2\pi\cdot\eta\cdot(d\mathfrak{W}/dx)^2 + 8\pi\cdot\eta\cdot\mathfrak{U}\cdot\mathfrak{W}\cdot(1 + \mathfrak{W}/2x) \right] \ . \qquad \text{(B.24)}$$

We search for the minimum of $\mathcal{L}$ using functions similar to Eq. (B.22) with an arbitrary parameter S. We then have

$$\mathcal{L}(S) = 3S/8 + \pi\cdot\eta\cdot[S^{-2} + S^{-4}\ln(9/5)]/2 \ .$$

If value of η is large ($\eta > 1$), the function in Eq. (B.24) is minimal if $S = (4\pi\eta)^{1/4}$. This is in accordance with the solution of a linearized problem. If the value of η is small ($\eta \ll 1$), Eq. (B.23) is minimal if $S = [(16\pi\eta/3)\ln(\frac{9}{5})]^{1/5}$. The boundary value of η is $\eta_* = (2/\pi)[(\frac{2}{3})\ln(\frac{9}{5})]^4 \simeq 0.015$. If the electron density is small ($n_e < 10^{23}$ cm^{-3}), then screening is connected with the nonlinear terms in Eqs. (B.18) and (B.20). If the density is large ($n_e > 10^{23}$ cm^{-3}), the screening is connected with the linear terms in Eqs. (B.18) and (B.20). The physical reason for this is easy to understand. If the electron density is large, then the relatively small perturbations are enough for full screening of a positive charge. These perturbations can be described with good accuracy by a linear approximation. If the electron density is small, its perturbations near the positive charge are great, and a linear approximation is insufficient for their descriptions.

For a numerical solution of the boundary problem, it is convenient to convert differential equations [Eqs. (B.18) and (B.20)] with boundary conditions [Eqs. (B.10) and (B.21)] into integral equations, which can be solved by iteration. Using the complete set of solutions, Eq. (B.22), of the linearized equations, Eqs. (B.18) and (B.20), we can write the formal solutions of these equations in the following form:

$$\mathfrak{U}(x) = (1 + Q)\exp(-y)\cos(y) - P\exp(-y)\sin(y) + \left(\frac{1}{4}\right)\int_0^\infty dy' \exp(-|y - y'|) \times [q(y')\sin|y - y'| - r(y')\cos(y - y')]$$

and

$$\mathfrak{W}(x) = (1 + Q)\exp(-y)\sin(y) + P\exp(-y)\cos(y) - \left(\frac{1}{4}\right)\int_0^\infty dy' \exp(-|y - y'|) \times [q(y')\cos(y - y') + r(y')\sin|y - y'|] \ , \qquad \text{(B.25)}$$

where

$$y \equiv Sx \ ,$$
$$S = (4\pi\eta)^{1/4} \ ,$$
$$q(y) = S\mathfrak{W}(S^2\mathfrak{W} - 2\mathfrak{U})/y \ ,$$
$$r(y) = S\mathfrak{W}(S^2\mathfrak{W} + 2\mathfrak{U})/y \ ,$$
$$Q \equiv -\left(\frac{1}{4}\right)\int_0^\infty dy \exp(-y) \times [q(y)\sin(y) - r(y)\cos(y)] \ ,$$

and

$$P \equiv \left(\frac{1}{4}\right)\int_0^\infty dy \exp(-y) \times [q(y)\cos(y) + r(y)\sin(y)] \ .$$

The equations are solved by iterations. Examples of solutions to Eq. (B.25) are shown in Fig. B.1. The dashed lines represent the space distribution of the modified potential $\mathfrak{U}(x)$, and the solid lines show the modified electron density $\mathfrak{N}(x) = 2\mathfrak{W}(x)[1 + \mathfrak{W}/2x]$.

Note the remarkable fact that the screening parameter depends on the background electron density according to

$$\lambda_q = S/a = [4\pi m e^2 n_0/\hbar^2]^{1/4} \ .$$

This dependence differs from the dependence of the Fermi screening parameter that is usually used in the theory of solids (see, e.g., Refs. 43 and 44):

$$\lambda_F = 2e m^{1/2} n_0^{1/6} \hbar^{-1} \ .$$

Let us consider the effects connected with the finiteness of the average electron energy. In this case, the result depends on the shape of the distribution function. The Fermi spectrum is of practical interest, but the solution has serious mathematical difficulties in this case.

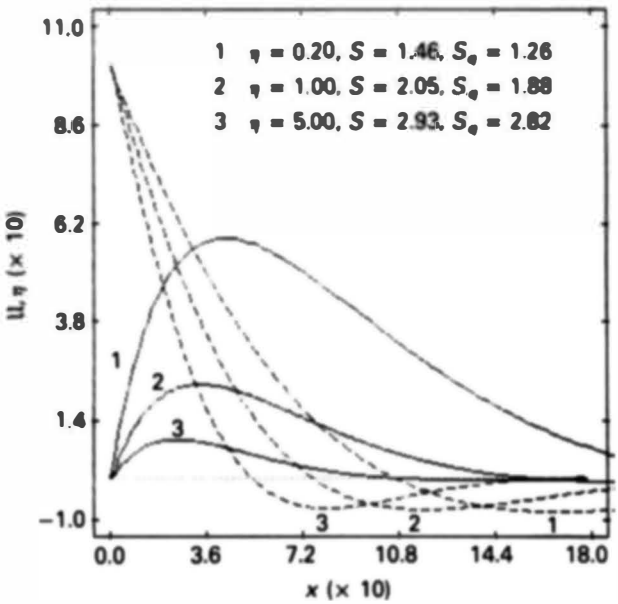

Fig. B.1. Distributions of the modified electron density (solid lines) and electrical potential (dashed lines) near the positive charge.

It is quite acceptable to use a distribution function as follows:

$$f(K) = 4\kappa K^2/\pi(K^2 + \kappa^2)^2 \ . \qquad \text{(B.26)}$$

This function is similar to the Fermi distribution in the range $K < \kappa$.

Let us insert Eq. (B.26) into Eq. (B.16). This yields

$$G(x,y) = (1/2\kappa^2)\cdot\{[1 + \kappa|x-y|]\exp[-\kappa|x-y|] - [1 + \kappa(x+y)]\exp[-\kappa(x-y)]\} \ . \qquad \text{(B.27)}$$

If $x > y$, this function has the form

$$G(x,y) = \kappa^{-2}\exp(-\kappa x)\,[(1 + \kappa x)sh(\kappa y) - \kappa y ch(\kappa y)] \ . \qquad \text{(B.28)}$$

Let us note that the Maxwell distribution function

$$f(K) = (4K^2/\pi^{1/2}\kappa^3)\exp[-(K/\kappa)^2]$$

yields a G function of the form

$$G(x,y) = (2/\kappa^2)\exp[-\kappa^2(x^2 + y^2)/4]\,sh(\kappa^2 xy/2) \ . \qquad \text{(B.29)}$$

Comparison of the two G functions [Eqs. (B.28) and (B.29)] shows that they are similar in the most important region, $x \simeq y$. In other words, the difference between the distribution function, Eq. (B.26), and the exponentially decreasing distributions does not lead to significant differences in the G functions. Therefore, we use a distribution function in the form of Eq. (B.26).

Let us consider the functions

$$\mathcal{W}_e(x) = \int_0^\infty dy\, I(x,y)sh(\kappa y)$$

and

$$\mathcal{W}_c(x) = \kappa\int_0^\infty dy\, y I(x,y)ch(\kappa y) \ .$$

The integral

$$\mathfrak{I}(x) = \int_0^x dy\, I(x,y)G(x,y) \qquad \text{(B.30)}$$

is determined by these functions as follows:

$$\mathfrak{I}(x) = \kappa^{-2}\exp(-\kappa x)\,[(1 + \kappa x)\mathcal{W}_s(x) - \mathcal{W}_c(x)] \ .$$

This [see Eq. (B.20)] method yields the equations for $\mathcal{W}_s(x)$ and $\mathcal{W}_c(x)$:

$$d^2\mathcal{W}_s/dx^2 - [\kappa^2 - 2\mathcal{U}(x)/x]\mathcal{W}_s(x) + 2\mathcal{U}(x)sh(\kappa x)/x = 0$$

and

$$d^2\mathcal{W}_c/dx^2 - [\kappa^2 - 2\mathcal{U}(x)/x]\mathcal{W}_c(x) + 2\kappa\mathcal{U}(x)ch(\kappa x) = 2\kappa^2\mathcal{W}_s(x) \ .$$

Note that these equations have the form of the Schrödinger equation. The term $2\mathcal{U}(x)/x$ corresponds to the potential hole, but effective energy κ^2 has a sign that corresponds to the bound states of the electrons. Formally, it leads to an increase in the free-electron density near a positive charge. The direct consequence of this increase is the effect of screening of the Coulomb potential of positive charge. According to Eq. (B.15), perturbations of the electron density are determined by the sum of Eq. (B.30) and the following:

$$\int_0^x dy\, I(x,y)\int_0^x dt\, I(x,t)G(x,t) \ . \qquad \text{(B.31)}$$

This nonlinear term plays an important role only in the case of a small electron density ($\eta < 0.015$). If $\eta > 0.015$ (correspondingly, $P > 0.25$ Mbar), the role of Eq. (B.31) in the sum of Eq. (B.15) is negligibly small. We can write, in this case,

$$d^2\mathcal{U}/dx^2 = 8\pi\eta\kappa^{-2}\exp(-\kappa x)\,[\kappa\mathcal{W}_s + (\mathcal{W}_s - \mathcal{W}_c)/x] \ .$$

Further steps are reduced to the search for a more or less convenient method to solve the corresponding boundary problems. One such method was described earlier.

Examples of the results are shown in Fig. B.2. The dashed lines represent the space distribution of the modified potential $\mathcal{U}(x)$, and the solid lines show the modified electron density $\mathfrak{N}(x) = 2\mathcal{W}(x)\,[1 + \mathcal{W}/2x]$.

Note the remarkable fact that the screening parameter increases if wave vector κ increases. The physical reason for this is easy to understand. If the electron's momentum increases, the uncertainty of its position decreases. Hence, the distance of the closest approach of electrons to a nucleus decreases. This effect is exactly opposite to the decrease in the Debye screening parameter with temperature increase.

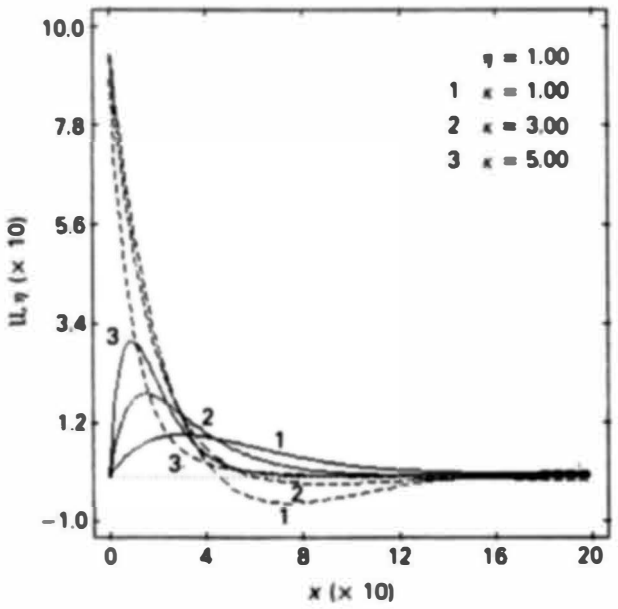

Fig. B.2. Distributions of the modified electron density (solid lines) and electrical potential (dashed lines) near the positive charge in the electron background with an average electron density $\eta = 1.0$ and with various values of average wave vector κ.

ACKNOWLEDGMENTS

I would like to thank S. A. Merkulov and A. B. Pankratov for helpful discussions.

REFERENCES

1. W. A. WILDHACK, "Proton-Deuteron Transformation as a Source of Energy in Dense Stars," *Phys. Rev.*, **57**, 81 (1940).

2. E. SCHATZMAN, "Thermo-Nuclear Reactions at High Densities (Degenerate and Non-Degenerate Gas)," *J. Phys. Radium*, **9**, 46 (1948).

3. E. E. SALPETER, "Nuclear Reaction in the Stars," *Phys. Rev.*, **88**, 547 (1952).

4. E. E. SALPETER, "Reactions of Light Nuclei and Young Contracting Starts," *Aus. J. Phys.*, **7**, 353 (1954).

5. Y. B. ZEL'DOVICH, "Nuclear Reactions in Cold Hydrogen at High Density," *Sov. Phys.: JETP*, **33**, 991 (1957).

6. E. E. SALPETER and H. M. VAN HORN, "Nuclear Reaction Rates at High Densities," *Astrophys. J.*, **55**, 183 (1969).

7. S. E. KOONIN and M. NAUENBERG, "Calculated Fusion Rates in Isotopic Hydrogen Molecules," *Nature*, **339**, 690 (1989).

8. A. J. LEGGETT and G. BAYM, "Can Solid-State Effects Enhance the Cold-Fusion Rate?," *Nature*, **340**, 45 (1989).

9. B. DELLEY, "Effect of Electronic Screening on Cold-Nuclear-Fusion Rates," *Europhys. Lett.*, **10**, *4*, 347 (1989).

10. A. J. LEGGETT and G. BAYM, "Exact Upper Bound on Barrier Penetration Probabilities in Many-Body Systems: Application to 'Cold Fusion,'" *Phys. Rev. Lett.*, **63**, *2*, 191 (1989).

11. F. MARCHESONI, C. PRESILLA, and F. SACCHETTI, "Pair Interaction Energy of Hydrogen Isotopes in Metallic Lattices. Estimate of Fusion Rates," *Europhys. Lett.*, **10**, *5*, 493 (1989).

12. Z. SUN and D. TOMANEK, "Cold Fusion: How Close Can Deuterium Atoms Come Inside Palladium," *Phys. Rev. Lett.*, **63**, *1*, 59 (1989).

13. M. SPRINGBORG, "On the Interactions Between Hydrogen and Palladium," *Europhys. Lett.*, **11**, *4*, 325 (1990).

14. S.-H. WEI and A. ZUNGER, "Stability of Atomic and Diatomic Hydrogen in icc Palladium," *Solid State Comm.*, **73**, *5*, 327 (1990).

15. J. L. FOWLER and J. E. BROLLEY, "Monoenergetic Neutron Techniques in the 10- to 30-MeV Range," *Rev. Mod. Phys.*, **28**, 103 (1956).

16. W. R. ARNOLD et al., "Cross Sections for the Reactions $D(d,p)T$, $D(d,n)He^3$, $T(d,n)He^4$, and $He^3(d,n)He^4$ Below 120 keV," *Phys. Rev.*, **93**, 483 (1954).

17. L. D. LANDAU and E. M. LIFSHITZ, *Course of Theoretical Physics, Vol. 3, Quantum Mechanics. Nonrelativistic Theory*, p. 673, Pergamon Press, Oxford (1977).

18. A. JAYARAMAN, "Recent Developments in Static High Pressure Research," *Rev. Mod. Phys.*, **55**, 65 (1983).

19. H. HORA, G. H. MILEY, L. CICCHITELLI, A. SCHARMANN, and W. SCHEID, "Nuclear Fusion in Host Lattices Discussed by the Model of a Nondegenerate Positive Hydrogen Isotope Ion Gas," *Proc. 5th Int. Conf. Emerging Nuclear Energy Systems*, Karlsruhe, Germany, July 3–6, 1989, G. KESSLER, Ed., World Scientific (1989).

20. H. HORA, G. H. MILEY, M. RAGHEB, and A. SCHARMANN, "Surface Models for Cold Fusion and Possibility of Multilayered Cells for Energy Production," *Proc. Cold Fusion Symp., 8th World Hydrogen Energy Conf.*, Honolulu, Hawaii, July 22–27, 1990, University of Hawaii.

21. H. HORA, L. CICCHITELLI, G. H. MILEY, M. RAGHEB, A. SCHARMANN, and W. SCHEID, "Plasma and Surface Tension Model for Explaining the Surface Effect of Tritium Generation at Cold Fusion," *Nuovo Cimento*, **12**, *3*, 393 (1990).

22. G. V. FEDOROVICH, "The Electron-Nuclear System of the E-Cell," *J. Phys. Condens. Matter*, **2**, 5077 (1990).

23. G. V. FEDOROVICH, "Features of the Coulomb Interaction in a Radiation Defect of the Hydride Crystal," *JTP Lett.*, **16**, 63 (1990).

24. G. V. FEDOROVICH, "The Coulomb Interaction in the E-Cell," *Sov. Phys.: Tech. Phys.*, **61**, *8*, 1 (1991).

25. G. V. FEDOROVICH, "The Coulomb Interaction in the E-Cell," *Physica B.*, **172**, 491 (1991).

26. G. V. FEDOROVICH, "The Tunnelling Effect in the Thomas-Fermi Model," *Physica Scripta*, **44**, 555 (1991).

27. G. V. FEDOROVICH, "Catalysis of Nuclear Fusion in Hydride Crystals at High Pressure," *Problems of Nuclear Science and Technics*, Theoretical and Applied Physics Series, No. 2, p. 34 (1991).

28. G. V. FEDOROVICH, "Quantum-Mechanical Screening," *Phys. Lett. A*, **164**, 149 (1992).

29. Landolt-Bornstein, Neue Serie, Gruppe III, Band 6, Table 3.3, Springer-Verlag, Berlin (1971).

30. J. S. BLAKEMORE, *Solid State Physics*, p. 606, Cambridge University Press (1985).

31. A. LUND and S. SCHLICK, "Trapped Electrons in Crystalline Media," *Res. Chem. Intermediates*, **11**, 37 (1989).

32. D. F. FENG and L. KEVAN, "Theoretical Models for Solvated Electrons," *Chem. Rev.*, **80**, 1 (1980).

33. L. KEVAN, S. SCHLICK, P. A. NARAYANA, and D. F. FENG, "Active Microwave Delay Line for Reducing the Dead Time in Electron-Spin Echo Spectrometry," *J. Chem. Phys.*, **75**, 1980 (1981).

34. T. R. TUTTLE and S. GOLDEN, "Solvated Electron Optical Absorbtion Spectra in Liquid Methylamide," *J. Chem. Soc. Faraday Trans. 2*, **78**, 1581 (1982).

35. P. GOMBAS, *Die statistische Theorie des Atoms und ihre Anwendungen*, p. 406, Springer, Vienna (1949).

36. S. FLUGGE, *Lehrbuch der Theoretischen Physik*, Vol. 4, p. 313, Springer-Verlag, Berlin (1964).

37. H. ESSEN, "Periodic Table of the Elements and the Thomas-Fermi Atom," *Int. J. Quantum Chem.*, **21**, 717 (1982).

38. L. D. LANDAU and E. M. LIFSHITZ, *Course of Theoretical Physics, Vol. 5, Statistical Physics*, p. 563, Pergamon Press, Oxford (1977).

39. S. S. SCHWEBER, *An Introduction to Relativistic Quantum Field Theory*, p. 842, Row, Peterson and Company, New York (1961).

40. G. A. KORN and Th. M. KORN, *Mathematical Handbook*, p. 830, McGraw-Hill, New York (1968).

41. R. G. NEWTON, *Scattering Theory of Waves and Particles*, p. 530, McGraw-Hill, New York (1966).

42. T.-Y. WU and T. OHMURA, *Quantum Theory of Scattering*, p. 358, Prentice-Hall, Englewood Cliffs, New Jersey (1962).

43. Ch. KITTEL, *Introduction to Solid State Physics*, p. 790, John Wiley & Sons, New York (1975).

44. J. M. ZIMAN, *Principles of the Theory of Solids*, p. 532, Cambridge University Press (1972).